

SOURCE OF GABA IN IMMATURE GLYCINERGIC SYNAPSES OF BRAINSTEM

SPATIOTEMPORAL PATTERNS OF PROTEINS ASSOCIATED WITH GABA SYNTHESIS
AND TRANSPORT IN THE DEVELOPING AUDITORY BRAINSTEM

BY SIYI MA, B. Sc.

A Thesis Submitted to the School of Graduate Studies in Partial Fulfilment of the
Requirements for the Degree Master of Science

McMaster University © Copyright by Siyi Ma, August 2019

McMaster University MASTER OF SCIENCE (2019) Hamilton, Ontario

TITLE: Spatiotemporal Patterns of Proteins associated with GABA Synthesis and Transport in the Developing Auditory Brainstem

AUTHOR: Siyi Ma, B. Sc. (McMaster University)

SUPERVISOR: Dr. Deda C. Gillespie

NUMBER OF PAGES: xii, 40

LAY ABSTRACT

Evolutionarily older parts of the mammalian brain, such as the brainstem, typically play little role in higher-order functions, but contain regulatory centers that are critically important for keeping the organism alive. As conventional wisdom has been that brainstem centers require fast inhibitory communication (mediated by the neurotransmitter glycine) to carry out their critical functions, an ongoing mystery lies in why many immature inhibitory neurons in the developing brainstem use the relatively slow inhibitory neurotransmitter, GABA. We and others have speculated that inhibitory neural circuits of the brainstem require GABA for maturation and/or refinement.

As a first step in addressing this question in the auditory brainstem, we looked for the cellular and molecular sources of GABA by performing antibody stains for various proteins known to be involved in GABA synthesis and transport. Our results suggest, somewhat surprisingly, that GABA in the immature brainstem likely arises from non-classical sources.

ABSTRACT

During an early developmental period, some glycinergic synapses in the brainstem and spinal cord release predominately GABA, which activates GABA_A receptors on the postsynaptic membrane. The function of this early GABAergic transmission is unknown but presumed to contribute to synapse maturation. Classically, the enzyme glutamic acid decarboxylase (GAD), which synthesizes GABA from glutamate, has been considered the sole source of GABA in neurons. GABAergic neurons typically express one or both of the two known isoforms of this enzyme, GAD65 and GAD67. However, co-transmitting synapses in the midbrain were recently reported to acquire GABA through other means – GABA transporters (GAT1 and GAT3) and/or aldehyde dehydrogenase (ALDH1A1).

To determine the source of GABA in immature glycinergic neurons of the auditory brainstem, we immunostained for GADs, GATs, and ALDH1A1, co-staining with markers for glial cell and synaptic terminals to verify cellular and subcellular location.

GAD65 was expressed in synaptic terminals whereas GAD67 was localized to neuronal cell bodies, proximal dendrites, and presumed synaptic terminals. However, during the peak period of GABA transmission in the first postnatal week, expression levels of both GAD65 and GAD67 were surprisingly low. Although GAT1 and GAT3 expression levels coincided with the peak period of GABA transmission, neither GAT was localized to neuronal cell bodies. In contrast, ALDH1A1 was expressed during the first postnatal week and was localized to neuronal cell bodies. These results suggest that immature glycinergic neurons of the auditory brainstem may not acquire GABA through classical GABA synthesis or GABA reuptake, but perhaps are able to synthesize GABA through the putrescine degradation pathway mediated by ALDH1A1.

ACKNOWLEDGEMENTS

I would like to thank my supervisor, Dr. Deda Gillespie, for always welcoming me into her office whenever I needed advice and thank you to all members of the Gillespie Lab for their help and especially for moral support. I would also like to thank Dr. Colin Nurse and Dr. Daniel Goldreich for serving on my supervisory committee. I am very grateful to my parents who have always supported me and are always there for me.

TABLE OF CONTENTS

1. Introduction	1
1.1 General Inhibitory Circuit Maturation.....	1
GABA and glycine are depolarizing during development.....	1
Change in neurotransmitter and receptor type	2
1.2 Circuitry of the superior olivary complex.....	3
Ventral cochlear nucleus (VCN).....	3
Nuclei of the trapezoid body (MNTB; LNTB; VNTB)	4
Lateral superior olive (LSO) and medial superior olive (MSO)	4
Superior paraolivary nucleus (SPN)	5
1.3 Refinement of MNTB-LSO pathway during development	5
1.4 Proteins involved in GABA synthesis and transport.....	6
Glutamic acid decarboxylases (GADs)	6
GABA transporters (GATs) and aldehyde dehydrogenase (ALDH1A1).....	7
2. Objective	7
3. Methods	8
Tissue collection	8
Immunohistochemistry	8
Antibody Characterization	10
Image acquisition and analysis.....	12
Planned experiments	12
4. Results.....	12
Spatiotemporal pattern of GAD65 and GAD67 in the developing SOC	12
GAD65	12
GAD67	13
Spatiotemporal pattern of GAT1 and GAT3 in the developing SOC	13
GAT1	13
GAT3	14
Spatiotemporal pattern of ALDH1A1 in the developing SOC.....	14

5. Figures	15
6. Discussion.....	30
GAD65 and GAD67 expression do not correlate with the known timeframe of GABAergic transmission in the SOC	30
Non-neurotransmitter roles for GABA	31
Neurons in the SOC do not express the GATs necessary for GABA uptake	31
GAT1 and GAT3 may be involved in GABA clearance in the SOC	31
ALDH1A1 is potentially expressed in SOC neurons.....	32
7. Troubleshooting	33
Reliability of Immunohistochemistry Studies	33
Glial Expression in the SOC.....	33
ALDH1A1 Antibody Specificity.....	33
8. Conclusion	34
REFERENCES	35

LIST OF FIGURES AND TABLES

Figure 1	Schematic illustration of coronal section through the superior olivary complex	3
Figure 2	Overview of GAD65-IR in the developing rat SOC and VCN	18
Figure 3	Overview of GAD67-IR in the developing rat SOC and VCN	19
Figure 4	Overview of GAT1-IR in the developing rat SOC and VCN.....	20
Figure 5	Overview of GAT3-IR in the developing rat SOC and VCN.....	21
Figure 6	Overview of ALDH1A1-IR in the developing rat SOC and VCN	22
Figure 7	High magnification confocal images of GAD65-IR, Syt2-IR, and GFAP-IR.....	23
Figure 8	High magnification confocal images of GAD67-IR and GFAP-IR.....	24
Figure 9	High magnification confocal images of GAD67-IR and NeuroTrace	25
Figure 10	High magnification confocal images of GAT1-IR, Syt2-IR and NeuroTrace	26
Figure 11	High magnification confocal images of GAT3-IR, Syt2-IR and NeuroTrace	27
Figure 12	High magnification confocal images of ALDH1A1-IR, GFAP-IR and NeuroTrace	28
Figure 13	High magnification confocal images of ALDH1A1-IR, Syt2-IR and NeuroTrace.....	29

Table 1 List of antibodies used	15
Table 2 Distribution and relative immunoreactivity of GAD65 in SOC and VCN based on visual inspection (– <i>absent</i> , + <i>weak</i> , ++ <i>moderate</i> , +++ <i>strong</i>)	21
Table 3 Distribution and relative immunoreactivity of GAD67 in SOC and VCN based on visual inspection (– absent, + weak, ++ moderate, +++ strong)	22
Table 4 Distribution and relative immunoreactivity of GAT-1 in SOC and VCN based on visual inspection (– absent, + weak, ++ moderate, +++ strong)	22
Table 5 Distribution and relative immunoreactivity of GAT-3 in SOC and VCN based on visual inspection (– absent, + weak, ++ moderate, +++ strong)	23
Table 6 Distribution and relative immunoreactivity of ALDH1A1 in SOC and VCN based on visual inspection (– absent, + weak, ++ moderate, +++ strong)	23

LIST OF ABBREVIATIONS

ALDH1A1	Aldehyde Dehydrogenase 1a1
CNS	Central Nervous System
DAO	Diamine Oxidase
E	Embryonic Day
GABA _A Rs	GABA _A Receptors
GADs	Glutamic Acid Dehydrogenases
GATs	GABA Transporters
GlyRs	Glycine Receptors
ILD	Interaural Level Difference
ITD	Interaural Time Difference
KCC2	K-Cl Cotransporter
LNTB	Lateral Nucleus of the Trapezoid Body
LOC	Lateral Olivocochlear
LSO	Lateral Superior Olive
MNTB	Medial Nucleus of the Trapezoid Body
MOC	Medial Olivocochlear
MSO	Medial Superior Olive
NKCC1	Na-K-Cl cotransporter
NMDARs	N-Methyl-D-Aspartate receptors
NTBs	Nuclei of the Trapezoid Body
P	Postnatal Day
PBS	Phosphate Buffered Saline
PLP	Pyridoxal Phosphate
RALDH	Retinaldehyde Dehydrogenase
SOC	Superior Olivary Complex
SPN	Superior olivary Nucleus

VCN	Ventral Cochlear Nucleus
VIAAT	Vesicular Inhibitory Amino Acid Transporter
VNTB	Ventral Nucleus of the Trapezoid Body

DECLARATION OF ACADEMIC ACHIEVEMENT

The developmental expression of GABA synthesizing proteins in the LSO project was first started by Chloe Bair-Marshall for her undergraduate thesis in Dr. Deda Gillespie's lab. I continued this project and examined the expression of GADs, GATs, and ALDH1A1 in all major nuclei in the auditory brainstem. I collected the rat brains with the help of Shane Simon from Dr. Deda Gillespie's lab. Tara Quigley, also from the lab, helped me with initial pilot immunostaining runs of GADs and imaging on the epifluorescence microscope. I sectioned all the brains and performed all subsequent immunostaining runs. I imaged the tissues on the confocal microscope and analyzed the immunoreactivity on ImageJ.

1. Introduction

1.1 General Inhibitory Circuit Maturation

The optimal workings of a neural circuit depend on a balance of excitation and inhibition. Although excitatory circuit development has been extensively studied, not as much is known about proper inhibitory circuit development. The two major inhibitory neurotransmitters in the brain are gamma-aminobutyric acid (GABA) and glycine (for review, see Ito, 2016). Both neurotransmitters are typically synthesized in the presynaptic terminals and packaged into synaptic vesicles via a vesicular inhibitory amino acid transporter (VIAAT). Upon arrival of an action potential at the presynaptic terminals, synaptic vesicles undergo exocytosis, releasing their neurotransmitter contents into the synaptic cleft where the neurotransmitters are free to bind to their respective receptors. GABA activates ionotropic GABA receptors (GABA_AR) and metabotropic GABA receptors (GABA_BRs) while glycine activates ionotropic glycine receptors (GlyRs). Binding of the respective ligand to the ionotropic receptor triggers the opening of a Cl⁻ selective pore, allowing Cl⁻ to enter/leave the cell. Distinct brain regions show preferential use of either GABA or glycine; however, some circuits utilize both. Mixed synapses are most often found during development (Dumoulin et al., 2001; Avila et al., 2013) and typically the neuron shifts to predominantly use one of the inhibitory neurotransmitters.

Inhibitory circuits undergo some interesting changes during refinement and maturation (for review, see Gamlin et al., 2018). First, GABA and glycine are initially depolarizing and switch to hyperpolarizing within the first two postnatal weeks. And second, some inhibitory neurons switch from preferentially utilizing one neurotransmitter type to another. A change in neurotransmitter type may also be accompanied by postsynaptic receptor changes. These changes are highly circuit dependent.

GABA and glycine are depolarizing during development

Both glycine and GABA are depolarizing during early postnatal development in many CNS regions, including the spinal cord, brainstem, cerebellum, and hippocampus (Avila et al., 2013) due to elevated intracellular Cl⁻ levels in immature neurons. Therefore, activation of GABA_ARs and GlyRs results in Cl⁻ efflux and subsequent depolarization. At early postnatal ages, the intracellular Cl⁻ concentration is controlled mainly by the activity of the Na-K-Cl cotransporter (NKCC1), which transports Cl⁻ into the neurons. As the neurons mature, they begin to express the K-Cl cotransporter (KCC2), which pumps Cl⁻ out of neurons. The upregulation of KCC2 expression lowers intracellular Cl⁻ concentration. This shift in Cl⁻ gradient changes the reversal potential of GABA_ARs and GlyRs, leading to Cl⁻ influx upon activation of these receptors, and results in hyperpolarization of the neuron.

Disrupting the switch from depolarizing to hyperpolarizing GABA/glycine can affect neuronal development. For example, induced early expression of KCC2 in *Xenopus* tectal neurons prevents maturation of glutamatergic synapses (Akerman and Cline, 2006). Similarly, NKCC1-knockdown in newborn granule cells of the mouse hippocampus decreases dendritic complexity and disrupts GABAergic and glutamatergic transmission (Ge et al., 2005). Furthermore, preventing the switch from depolarizing to hyperpolarizing GABA can affect ocular dominance plasticity (Kanold and Shatz, 2006).

Change in neurotransmitter and receptor type

Another phenomenon that occurs during development is a change in synapse phenotype. In the spinal cord and brainstem, inhibitory neurons most commonly shift from using predominantly GABA or mixed GABA/glycine to predominantly glycine (for review, see Gamlin et al., 2018). A change in synapse phenotype can involve changes in presynaptic vesicles, changes in postsynaptic receptor expression, or both pre- and postsynaptic changes ((Kotak et al., 1998; Korada and Schwartz, 1999; Nabekura et al., 2003). The functional significance of a change in synapse phenotype is still unclear, but the timing and energetic cost of this change suggests that a change from predominantly GABAergic to predominantly glycinergic transmission is important for the refinement of this pathway. The synthesis of molecules and trafficking uses 25% of the total energy consumed by the brain (Harris et al., 2012). Drawing parallel from excitatory circuits, the insertion of postsynaptic glutamate receptors can double the energy consumption of the synapse. Therefore, we speculate that it would be more energetically costly for a synapse to alter its phenotype rather than maintaining the same phenotype, but that this trait has not been selected against in immature MNTB inputs because the trait is favorable to the refinement of this pathway.

1.2 Circuitry of the superior olivary complex

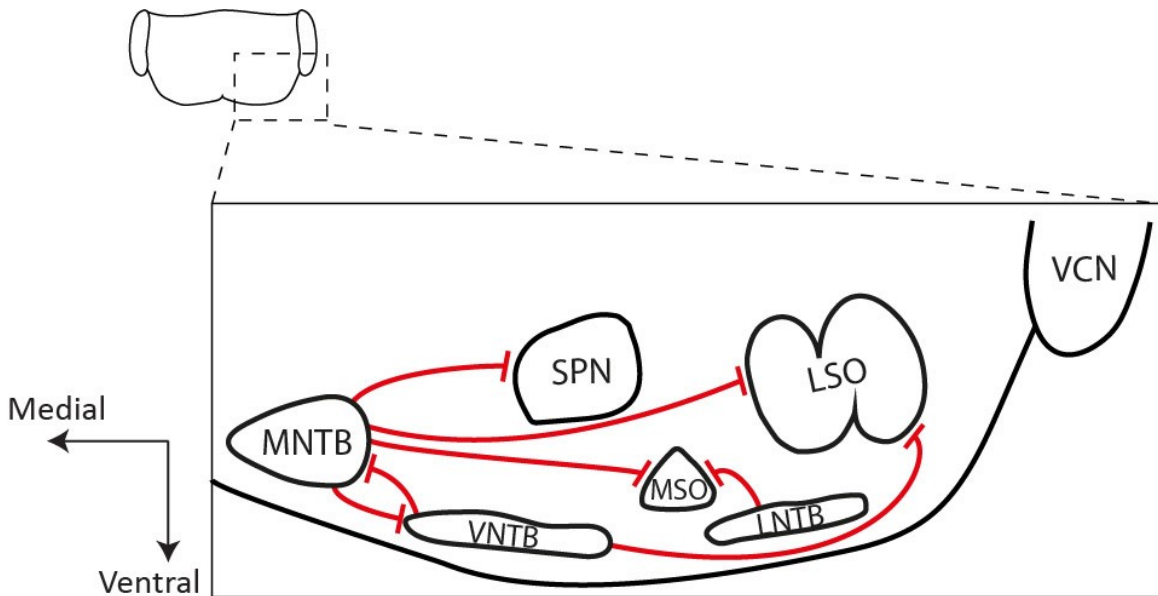


Figure 1 Schematic illustration of coronal section through the superior olivary complex (SOC) of rat, with inhibitory circuits highlighted (red). AVCN: anterior ventral cochlear nucleus; LNTB: lateral nucleus of the trapezoid body; LSO: lateral superior olive; MNTB: medial nucleus of the trapezoid body; MSO: medial superior olive; SPN: superior paraolivary nucleus; VNTB: ventral nucleus of the trapezoid body.

The superior olivary complex (SOC) is a cluster of nuclei in the ventral brainstem that processes auditory information from the two ears (Boudreau and Tsuchitani, 1968; Caird and Klinke, 1983). The nuclei of the trapezoid body (NTBs) – medial, lateral, and ventral – are sources of local inhibition within the complex while the lateral and medial superior olives (LSO and MSO), as well as the superior paraolivary nucleus (SPN) serve as the main outputs of the SOC by integrating excitatory information from ventral cochlear nuclei (VCN) with inhibitory information from the NTBs. The SOC is an ideal area to study development of inhibitory circuits due to the numerous, large inhibitory projections in this region (Fig. 1).

Ventral cochlear nucleus (VCN)

The VCN is the main excitatory input to the SOC and consists of a magnocellular region surrounded by a granular cell domain (GCD) (for review, see Rubio, 2018). In the

magnocellular region, spherical and globular bushy cells receive excitatory input from the auditory nerve fibers. The bushy cells provide the major excitatory inputs to the SOC. The other major cell type in the magnocellular region are stellate cells (multipolar cells): T-stellate cells and D-stellate cells (Doucet and Ryugo, 2006). T-stellate cells, which are glutamatergic, project widely through the SOC, and to upstream auditory pathway targets. D-stellate cells, which are glycinergic, provide inhibition within the VCN.

Nuclei of the trapezoid body (MNTB; LNTB; VNTB)

The MNTB receives excitatory input from the contralateral VCN. VCN input terminates on the MNTB soma, forming the largest synapse of the mammalian CNS, known as the Calyx of Held (Forsythe, 1994). These synapses allow for high fidelity excitatory transmission from the contralateral VCN. In the mature brain, MNTB neurons send glycinergic inputs to the LSO, SPN, and VNTB; however, during development, the MNTB inputs are GABAergic (Kotak et al., 1998; Korada and Schwartz, 1999; Nabekura et al., 2003). The LNTB receives excitatory input from the ipsilateral VCN and provides the main inhibitory input to MSO (Cant and Hyson, 1992; Spirou et al., 1998). The VNTB contains two populations of neurons: one comprised of choline acetyltransferase-positive neurons that are part of the medial olivocochlear (MOC) efferent feedback system (Darrow et al., 2012) and another comprised of glycinergic neurons that serve as local inhibitory neurons within the SOC. The glycinergic VNTB neurons project to ipsilateral LSO and contralateral LNTB (Warr and Beck, 1996). There is also a reciprocal inhibitory connection between MNTB and VNTB ((Kuwabara et al., 1991).

Lateral superior olive (LSO) and medial superior olive (MSO)

The principal cells of the LSO receive converging inputs from the two ears – excitatory inputs (glutamatergic) from the ipsilateral VCN and inhibitory inputs (GABA/glycinergic) from the contralateral VCN through the MNTB. The precise alignment of these inputs critically underlies the ability of the LSO to detect differences in sound intensity between the ears (Boudreau and Tsuchitani, 1968). The LSO contains many cell types (Helfert and Schwartz, 1987). The principal neurons, the major cell type, project to the inferior colliculus with information about interaural level differences (ILDs). The lateral olivocochlear neurons project to the cochlea as part of the lateral olivocochlear complex (LOC) (Jenkins and Simmons, 2006).

The MSO also receives direct bilateral excitatory inputs from both cochlear nuclei, calculates interaural time differences (ITDs), and projects to the inferior colliculus. In addition, it receives inhibitory glycinergic inputs from the MNTB and LNTB that are implicated in ITD processing (Grothe et al., 2010).

Superior paraolivary nucleus (SPN)

The SPN neurons have large somas and a multipolar dendritic organization. Unlike neurons of other nuclei in the SOC, the SPN neurons do not fire for the duration of the sound stimulus due to a powerful glycinergic input from the MNTB and fire when sound stimulus terminates (Kadner et al., 2006; Kopp-Scheinflug et al., 2011).

1.3 Refinement of MNTB-LSO pathway during development

Although synaptic inputs from the MNTB are functional as early as embryonic day 18 (E18) (Kandler and Friauf, 1995), the MNTB-LSO pathway undergoes many changes during the first three postnatal weeks. First, MNTB inputs evoke depolarizing responses in LSO neurons, rather than hyperpolarizing responses up until P7 and become hyperpolarizing thereafter (Kandler and Friauf, 1995, Ehrlich et al., 1999). Second, developing MNTB terminals switch from predominately GABAergic to glycinergic during the first two postnatal weeks. There is a change in both presynaptic vesicle content and postsynaptic receptor expression (Kotak et al., 1998; Korada and Schwartz, 1999; Nabekura et al., 2004). Third, the MNTB terminals also exhibit a transient glutamate release during the first postnatal week that predominantly acts on N-Methyl-D-Aspartate receptors (NMDARs) (Gillespie et al., 2005, Case et al., 2013). These changes are followed by anatomical pruning of the MNTB inputs between the second and third postnatal week (Sanes and Siverls, 1991; Sanes and Takács, 1993).

All of these events are thought to be important for the refinement of the MNTB-LSO pathway as they all coincide with the time of MNTB-LSO synapse elimination and strengthening (Kim and Kandler, 2003). When glutamate transmission is disrupted in the MNTB-LSO pathway, the pathway fails to undergo normal refinement (Noh et al., 2010), suggesting that glutamate-dependent depolarization is necessary for refinement. Lee et al. (2016) showed that KCC2-knockdown mice, in which GABA/glycine remains excitatory beyond the second postnatal week, displayed proper synaptic maturation and refinement; however, we do not know whether premature expression of KCC2, in which GABA/glycine would prematurely switch to being inhibitory, would affect circuit refinement in the brainstem. Evidence from work done in *Xenopus* and mouse hippocampus suggests that a premature switch of GABA/glycine from depolarizing to hyperpolarizing disrupts GABAergic and glutamatergic refinement (Ge et al., 2005; Akerman and Cline, 2006).

There is current no direct evidence that GABAergic transmission is necessary for refinement of the MNTB-LSO pathway, but we can hypothesize based on several unique properties of immature GABAergic signalling. First, GABA currents have slower decay kinetics than glycine currents (Nabekura et al., 2003) Since LSO neurons must properly integrate the excitatory input from the VCN with inhibitory input from the MNTB, the

slow GABA kinetics may be important for providing the cell with a broader window of coincidence detection between the inputs. Slow GABA kinetics may also be important for relieving the Mg^{2+} block for activation of NMDARs. NMDARs are the major contributor of the excitatory postsynaptic current in both the MNTB-LSO pathway and the VCN-LSO pathway during the first postnatal week, coinciding with the period of peak GABAergic transmission from the MNTB (Case and Gillespie, 2011; Case et al., 2011). GABA depolarization can also elicit long-lasting intracellular calcium transients due to their slower kinetics while glycine cannot (Kullmann et al., 2002). These calcium transients result from activation of postsynaptic L-type voltage-gated calcium channels (Kullmann et al., 2002) and may be important for proper refinement as Cav1.3-knockout (KO) mice displayed perturbed refinement in the MNTB-LSO pathway at P10-12 (Hirtz et al., 2012). Intracellular calcium cascades can activate many intracellular signalling pathways that promote dendrite branch formation and growth (Konur and Ghosh, 2005). Thus, calcium transients that result from GABA release could be involved in synapse maturation. Second, GABA can activate metabotropic GABA_BRs to modulate presynaptic release during development. Activation of GABA_BRs can hyperpolarize the presynaptic terminal and reduce vesicular release. Continuous focal application of GABA but not glycine induced synaptic depression in the MNTB-LSO pathway (Chang et al., 2003). In addition, MNTB fiber stimulation before hearing onset also activated presynaptic GABA_BRs in the MNTB-MSO pathway (Hassfurth et al., 2010). Because GABA/glycine is depolarizing during the first postnatal week, modulation of presynaptic release by GABA may be necessary to prevent excitotoxicity in the postsynaptic cell.

1.4 Proteins involved in GABA synthesis and transport

The MNTB-LSO pathway is predominantly glycinergic in its mature state but predominantly GABAergic in its immature state (Kotak et al., 1998; Korada and Schwartz, 1999; Nabekura et al., 2004). To further our understanding of the functional significance of the GABA to glycine switch, we must first look at the mechanism for synthesis and transport of GABA.

Glutamic acid decarboxylases (GADs)

Glutamic acid decarboxylase (GAD) is an enzyme that synthesizes GABA from glutamate when it is bound to the co-factor pyridoxal phosphate (PLP) (Roberts and Frankel, 1951). There are two forms of the enzyme, GAD65 and GAD67, derived from two genes, that are named for their molecular weights (Erlander et al., 1991). These two forms differ in their molecular size, antigenicity, cellular location, and interaction with PLP. In the rat cerebral cortex, GAD65 is expressed in synaptic terminals and GAD67 is expressed in cell bodies, proximal dendrites, and terminals (Kaufman et al., 1991).

Whereas GAD67 exist mostly as a constitutively active holoenzyme, GAD65 is only partly saturated with PLP (Erlander et al., 1991; Kaufman et al., 1991). GAD65-KO mice appear normal but are prone to seizure (Asada et al., 1996). Tian et al. (1999) recorded retinal ganglion cells and hippocampal pyramidal cells from GAD65-KO mice and found that while the miniature responses did not differ between wildtype and KO, frequency and amplitude responses from sustained stimulation was reduced in the KOs. GAD67-KO is perinatally lethal due to a severe cleft palate (Asada et al., 1997). These evidence suggests that GAD65 is primarily responsible for GABAergic transmission while GAD67 maintains baseline GABA levels.

GABA transporters (GATs) and aldehyde dehydrogenase (ALDH1A1)

GABA transporters (GATs) are GABA:sodium symporters that regulate extracellular GABA concentrations (Borden, 1996). Because no enzymes are known to degrade GABA in the synaptic cleft, clearance of GABA depends on GAT expression on neurons or astrocytes to recycle GABA. GAT1 and GAT3 are the most widespread GATs throughout the brain (Ikegaki et al., 1994). Like the GADs, GATs have distinct cellular expression patterns that differ between brain regions (for review, see Scimemi, 2014). GAT1 has been detected in synaptic terminals, axons, proximal dendrites, and astrocytes, while GAT3 is generally expressed in astrocytes adjacent to synapses. GAT1 expression in synaptic terminals suggests that either GABA can be directly recycled back into the neuron following release and perhaps serve as a source of GABA. Tritsch et al. (2014) reported that in midbrain dopamine neurons that co-release GABA and dopamine, GATs are required for sustained GABAergic transmission. However, even though the neurons can take up GABA, GABA production is still necessary. As an alternative to the classical GABA synthesis pathway via GADs, GABA can also be synthesized as a part of the putrescine degradation pathway by the enzymes ALDH1A1 and diamine oxidase (DAO) (Seiler and Al-Therib, 1974). (Kim et al., 2015) provided evidence that ALDH1A1 may be involved in synthesis of GABA in midbrain dopaminergic neurons.

With the rise in discovery of synapses that co-release multiple neurotransmitters, we should re-evaluate our previous conception of relying on GADs as a marker for GABAergic neurons.

2. Objective

Classically, GAD65 and GAD67 have been considered the sole source of GABA in neurons. However, previous immunohistochemistry (IHC) studies done by the lab have found no GAD immunoreactivity in immature MNTB neurons. To determine the source

of GABA in immature glycinergic terminals of the auditory brainstem, we examined the spatiotemporal patterns of GAD65, GAD67, GAT1, GAT3, and ALDH1A1 in all major nuclei of the SOC and VCN.

3. Methods

Tissue collection

All animal procedures were performed in accordance with the Canadian Council on Animal Care guidelines and were approved by the Animal Research Ethics Board of McMaster University. Sprague-Dawley rats aged postnatal day 0/1 (P0/1), P4/5, P8/9, P12/13, P16/17, P20/21, P24/25, and P28/29 from the same litter were euthanized with sodium pentobarbital (120 mg/kg) and transcardially perfused with 0.1 M phosphate-buffered saline (PBS) followed by cold 10% formalin or 4% paraformaldehyde. Brains were postfixed for 4-5 hours and cryoprotected in 30% sucrose in PBS until time of sectioning. The brains were processed within a month from the collection of the P28/29 brain.

Immunohistochemistry

Coronal sections containing the SOC were cut at 30 μ m on a freezing microtome and collected into PBS-filled wells. Sections were then stained for either GAD65, GAD67, GAT1, GAT3, or ALDH1A1 and counterstained with NeuroTrace 640/660 (a fluorescent nissl stain), to visualize neuronal cell bodies. All brains from a given litter were cut, stained, and imaged at the same time to reduce artifacts that might arise from differences in the processing workflow. For each protein localization, two litters were used. Additional P5, P13, P16, and P21 brains were collected for co-immunostaining with synaptotagmin 2 (Syt2), a marker for synaptic terminals in the brainstem (Fox and Sanes, 2007), and glial fibrillary acidic protein, a marker for astrocytes and counterstained with NeuroTrace 640/660.

All IHC was performed on free-floating sections at 4°C. Tissue sections were blocked in a solution containing 5% normal serum and 0.5% Triton X-100 in PBS for 15 hours, incubated in primary antibodies diluted in PBS or 5% NDS in PBS for 24 hours, incubated in secondary antibodies diluted in PBS or 5% NDS for 20 hours, and counterstained with NeuroTrace 640/660 for 1 hour. 0.5% BSA was also added to the buffer solution if the primary antibody host was mouse. Sections were washed 3 times in PBS between each step and before mounting and coverslipping. Non-hardening VectorShield antifade mounting medium (Cat # H-1000) was used and the slides were sealed with clear nail polish. For each age tested, a primary delete for each protein was

included as control. Additional controls were conducted for co-immunostains to evaluate possible antibody-antibody interaction.

Antibody Characterization

Table 1 List of antibodies used

Antigen	Dilution	Host	Manufacturer and Catalogue #	Antibody Characterization
ALDH1A1	1:200	Rabbit, polyclonal	Abcam ab23375	Discontinued*
GAD 65	1:200	Mouse, monoclonal	DSHB GAD-6	Initial Publication: (Chang and Gottlieb, 1988)
GAD 67	1:500	Mouse, monoclonal	Millipore MAB5406	(Fong et al., 2005) Immunoblot shows one distinct band at 67 kDa
GAT1	1:500	Rabbit, polyclonal	Millipore AB1570	PreadSORption controls: (Johnson et al., 1996)
GAT3	1:1000	Guinea Pig, polyclonal	SySy 274 304	Manufacturer Datasheet: Synthetic peptide corresponding to a.a. 612-627 of mouse GAT3
GFAP	1:500	Chicken, polyclonal	Millipore AB5541	Manufacturer's Datasheet: Produced from purified bovine GFAP and recognizes human, rat, and mouse GFAP
Syt2	1:500	Mouse, monoclonal	DSHB znp-1-c	Initial Publication: (Trevarrow et al., 1990)

* see discussion

Fluorophore	Dilution	Host	Target	Manufacturer and Catalogue #
Al 488	1:500	Donkey	Mouse	Jackson ImmunoResearch 715-545-151
Cy 3	1:500	Donkey	Mouse	Jackson ImmunoResearch 715-165-151
Cy 3	1:500	Donkey	Chicken	Jackson ImmunoResearch 703-165-155
Al 488	1:500	Donkey	Rabbit	Jackson ImmunoResearch 711-545-152
Cy 3	1:500	Donkey	Guinea Pig	Jackson ImmunoResearch 706-165-148

Image acquisition and analysis

Images were acquired on the confocal microscope (Leica SP8). For visual inspection of relative levels of immunoreactivity, low magnification images of the SOC and VCN were collected using a 20X air objective lens (NA 0.75) to compare overall intensity of different nuclei across development. Acquisition settings were kept constant for all images acquired within a staining run. For co-localization, images were collected using a 63X oil objective lens (NA 1.4) at Nyquist sampling with sequential imaging of each channel. All images were converted to tiff files and raw, unaltered images were analyzed on ImageJ.

Planned experiments

Due to time constraints, I did not finish all the experiments that I planned to do. For each protein in question, it would be ideal to have data from at least 3 litters. For colocalization experiments, I have not co-stained GAT1 or GAT3 with GFAP and GAD67 with Syt2. In addition, I also planned to co-stain ALDH1A1 with tau, a marker for axons.

4. Results

A summary of the developmental expression of GAD65, GAD67, GAT1, GAT3, and ALDH1A1 is given in Tables 2-6 (also see Figs. 2-6). The brightness of all figures has been artificially brightened for visualization purposes only.

Spatiotemporal pattern of GAD65 and GAD67 in the developing SOC

Overall, the SOC and VCN displayed prominent GAD immunoreactivity after P8/9 that remained elevated in the LSO, VNTB, and VCN until P28/29 (Table 2-3; Fig 2-3). GAD65-IR was detected in synaptic terminals, as indicated by colocalization with Syt2-IR (Fig 7f) while GAD67-IR was detected in a subset of neuronal cell bodies (Fig 9C, F, I), most striking in the LSO (Fig 9C), but also in the neuropil.

GAD65

GAD65-IR was weakly detected in the SPN during the first postnatal week but absent elsewhere in the SOC (Figs. 2A-B). GAD65-IR was evident in the LSO and VCN by P8/9 and VNTB by P12/13 (Figs. 2C-D). In the LSO, GAD65-IR was more diffuse early on and became more punctate later. VNTB showed very strong immunoreactivity in the third postnatal week, particularly in the lateral VNTB (Figs. 2F-H). In the VCN, GAD65-IR

was homogeneous within the nuclei until the third postnatal week, when a stronger signal was detected in the superficial layer (Fig 2F'-H'). GAD65-IR was virtually absent in the MNTB at all ages. The SPN, MSO, and LNTB showed weak immunoreactivity that did not vary much between the ages.

GAD65-IR in the LSO had a punctate pattern and was confined to the neuropil (Fig. 7F). GAD65-IR did not overlap with GFAP-IR (Fig. 7F). All regions positive for GAD65-IR were also positive for Syt2-IR, but perisomatic Syt2-IR did not show GAD65-IR (Fig. 7C). Presumed LSO cell bodies did not exhibit GAD65-IR (Fig 7D-F). The spatial pattern of GAD65-IR was similar between all SOC nuclei and VCN (data not shown).

GAD67

GAD67-IR was not detected in the SOC and VCN at P0/1 (Fig 3A, A'). The LSO and VCN exhibited weak immunoreactivity beginning at P4 and became more apparent in the older ages (Fig 3B-H). In the other nuclei, GAD67-IR was seen later in the second postnatal week and increased until P28/29 (Fig 3C-H). GAD67-IR in LSO cell bodies was more numerous in the lateral limb (Fig 3E-H). Like GAD65, GAD67-IR was virtually absent in the MNTB at all ages. The MSO and LNTB showed weak immunoreactivity that did not vary between the ages. The neuropil region dorsal to the SPN exhibited strong immunoreactivity from P8/9 to P28/29.

LSO cell bodies and proximal dendrites exhibited very strong GAD67-IR while GAD67-IR was weak and diffuse in VCN and VNTB cell bodies (Fig. 8C, F, I). In addition to positive GAD67-IR in a subset of neuronal cell bodies, GAD67-IR was also visible in the neuropil. GAD67-IR in the neuropil did not overlap with GFAP-IR (Fig 9C, F). The spatial pattern of GAD67-IR was similar between all SOC nuclei and VCN (data not shown).

Spatiotemporal pattern of GAT1 and GAT3 in the developing SOC

While GAT3-IR was visible in the LSO, MSO, MNTB, and SPN at birth and most intense in all nuclei at P4/5, GAT1-IR was not obvious until P8/9 and peaked around P12/13 (Table 4-5; Fig 4-5). By P24/25, both GAT1 and GAT3 signals were virtually absent (Fig 4-5G). Both GAT1-IR and GAT3-IR were observed in the neuropil but did not overlap with Syt2-IR (Fig 10-11D, H)

GAT1

GAT1-IR was not detected in the SOC and VCN at P0/1 (Fig 4A, A'). At P4/5, weak GAT1-IR was detectable in the LSO, MSO, SPN, MNTB, and VCN (Fig 4B, B'). By P8/9, most of the SOC and VCN are strongly labelled and the intensity increases until its peak

around P12/13 to P16/17 (Fig 4C-E). After P16/17, GAT1-IR intensity decreases to almost background levels (Fig 4F-H). From P4/5 to P12/13, GAT1-IR was very patchy within the SOC nuclei, with no apparent pattern (Fig 4B-D). In general, GAT1-IR intensity patterns did not vary much between nuclei.

GAT1-IR in the LSO and MNTB was very diffuse aside from a few sparse bright puncta (Fig 10A, E) and was localized in the neuropil (Fig 10D, H). GAT1-IR did not overlap with Syt2-IR (Fig 10D, H). The spatial pattern of GAT1-IR was similar between all SOC nuclei and VCN (data not shown).

GAT3

GAT3-IR displayed a similar patchiness to GAT1-IR although the patchiness was persistent in all ages. GAT3-IR was detectable in the LSO, MSO, MNTB, SPN, and VCN soon after birth at P0/1 and the intensity peaks by P4/5 in all nuclei (Fig 5A-B). GAT3-IR remains strong in the MNTB, VNTB, and VCN until after P24/5 while the immunoreactivity decreases in the LSO, MSO, MNTB, and SPN after P8/9. Although GAT3-IR in the VCN was initially homogeneous throughout the VCN in younger ages (Fig 5A'-E'), the signal remained in the superficial layer after P16/17 but was absent elsewhere in the nucleus (Fig 5F'-H').

GAT3-IR in the LSO and MNTB was very abundant in the neuropil. The patchiness seen in lower resolution images was also visible at higher magnification (Fig 11A, E). Co-immunostain of Syt2 and GAT3 showed clear separation between where they are expressed (Fig 11D, H). The spatial pattern of GAT3-IR was similar between all SOC nuclei and VCN (data not shown).

Spatiotemporal pattern of ALDH1A1 in the developing SOC

All nuclei displayed strong ALDH1A1-IR at P0/1 that persist until P8/9 (Fig 6A-C). After P8/9, ALDH1A1-IR decreases drastically (Table 6; Fig 6). In SOC nuclei, the ALDH1A1-IR appeared to be confined in fibrillar structures that ran through the nuclei (MNTB) or surrounded the nuclei (LSO). In the VCN, ALDH1A1-IR was weak and limited to the superficial layer.

The LSO and MNTB exhibited fibrillar ALDH1A1-IR in the neuropil and diffuse immunoreactivity in the cytoplasm (Fig 12A, E). ALDH1A1-IR in the neuropil does not overlap with either GFAP-IR or Syt2-IR (Fig 12D, G; Fig 13D, H). The spatial pattern of ALDH1A1-IR was similar between all SOC nuclei and VCN (data not shown).

5. Figures

Table 2 Distribution and relative immunoreactivity of GAD65 in SOC and VCN based on visual inspection (– *absent*, + *weak*, ++ *moderate*, +++ *strong*)

	GAD65							
	P0/1	P4/5	P8/9	P12/13	P16/17	P20/21	P24/25	P28/29
VCN	–	–	+	+	+	++	++	++
LSO	–	+	++	++	+++	++	+	++
MSO	–	–	–	–	+	+	–	+
MNTB	–	–	–	–	–	–	–	+
VNTB	–	–	+	++	++	+++	+++	+++
LNTB	–	–	+	+	+	+	+	+
SPN	+	+	+	+	+	++	–	+

Table 3 Distribution and relative immunoreactivity of GAD67 in SOC and VCN based on visual inspection (– *absent*, + *weak*, ++ *moderate*, +++ *strong*)

	GAD67							
	P0/1	P4/5	P8/9	P12/13	P16/17	P20/21	P24/25	P28/29
VCN	–	+	++	+	++	++	++	+++
LSO	–	+ ^c	+++ ^c	++ ^c	+++ ^c	+++ ^c	+++ ^c	+++ ^c
MSO	–	–	++	+	+	+	+	+
MNTB	–	–	–	–	+	+	+	+
VNTB	–	–	+	+	++	++	++	+++
LNTB	–	–	+	–	+	+	+	+
SPN	–	–	+	+	+	+	+	++

^c Immunoreactivity in cell bodies

Table 4 Distribution and relative immunoreactivity of GAT-1 in SOC and VCN based on visual inspection (– absent, + weak, ++ moderate, +++ strong)

	GAT-1							
	P0/1	P4/5	P8/9	P12/13	P16/17	P20/21	P24/25	P28/29
VCN	–	+	++	+++	++	++	–	+
LSO	–	+ ^a	++ ^a	+++ ^a	+++	+	–	+
MSO	–	+	++	+++	++	++	+	+
MNTB	–	+ ^a	+++ ^a	+++	++	+	–	+
VNTB	–	–	+	+++	++	+	+	+
LNTB	–	–	–	+++	++	+	+	–
SPN	–	+ ^a	+ ^a	+++ ^a	++	+	–	–

^a uneven, patchy immunoreactivity

Table 5 Distribution and relative immunoreactivity of GAT-3 in SOC and VCN based on visual inspection (– absent, + weak, ++ moderate, +++ strong)

	GAT-3							
	P0/1	P4/5	P8/9	P12/13	P16/17	P20/21	P24/25	P28/29
VCN	–	+++	+++	+++	+++	++	+	+
LSO	+++ ^a	+++	++	++	+	+	–	–
MSO	++	+++	+	+	++	+	–	–
MNTB	+++ ^a	+ ^a	+ ^a					
VNTB	–	+++	++	++	++	++	+	+
LNTB	–	+++	++	++	+	++	–	–
SPN	+++ ^a	+++ ^a	+ ^a	+ ^a	+ ^a	+ ^a	–	–

^a uneven, patchy immunoreactivity

Table 6 Distribution and relative immunoreactivity of ALDH1A1 in SOC and VCN based on visual inspection (– absent, + weak, ++ moderate, +++ strong)

	ALDH1A1							
	P0/1	P4/5	P8/9	P12/13	P16/17	P20/21	P24/25	P28/29
VCN	+++	+++	+++	++	+	+	–	–
LSO	+++ ^a	+++ ^a	+++ ^a	+	++	++	+	–
MSO	+++ ^b	+++ ^b	+++ ^b	++	++	+	+	–
MNTB	+++ ^b	+++ ^b	+++ ^b	+ ^b	+ ^b	+ ^b	+ ^b	–
VNTB	+++ ^b	+++ ^b	++ ^b	++ ^b	+ ^b	+ ^b	–	–
LNTB	+++ ^b	+++ ^b	+++ ^b	+ ^b	++ ^b	+ ^b	–	–
SPN	++	++	++	+	+	+	–	–

^a uneven, patchy immunoreactivity

^b immunoreactivity in long fibers across nucleus

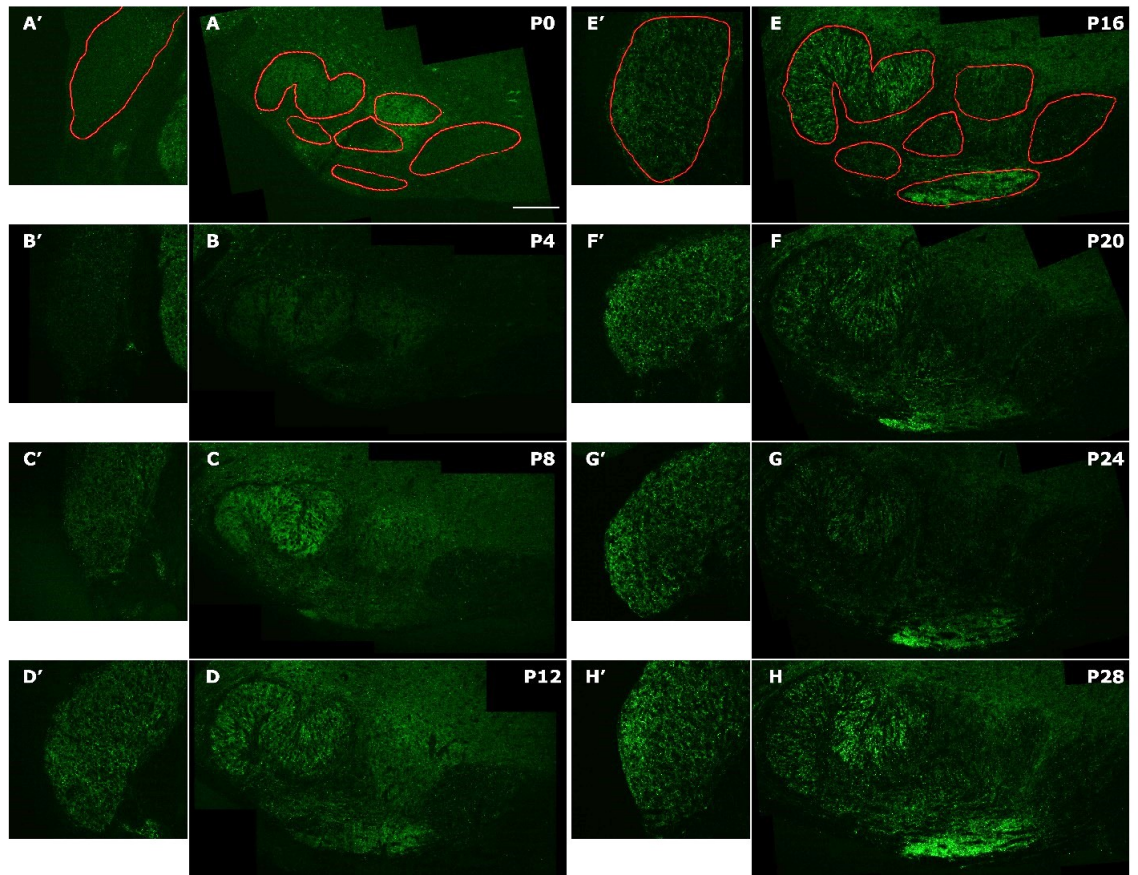


Figure 2 Overview of GAD65-IR in the developing rat SOC and VCN between P0 and P28. SOC nuclei and VCN are outlined in red (**A**, **A'**, **E**, **E'**). GAD65-IR is absent in all nuclei during the first postnatal week. Almost no GAD65-IR is detected in the MNTB at any ages. Labeling in the LSO, VNTB, and VCN is detectable in the second postnatal week and increases with age (**c**). Scale bar = 200 μm.

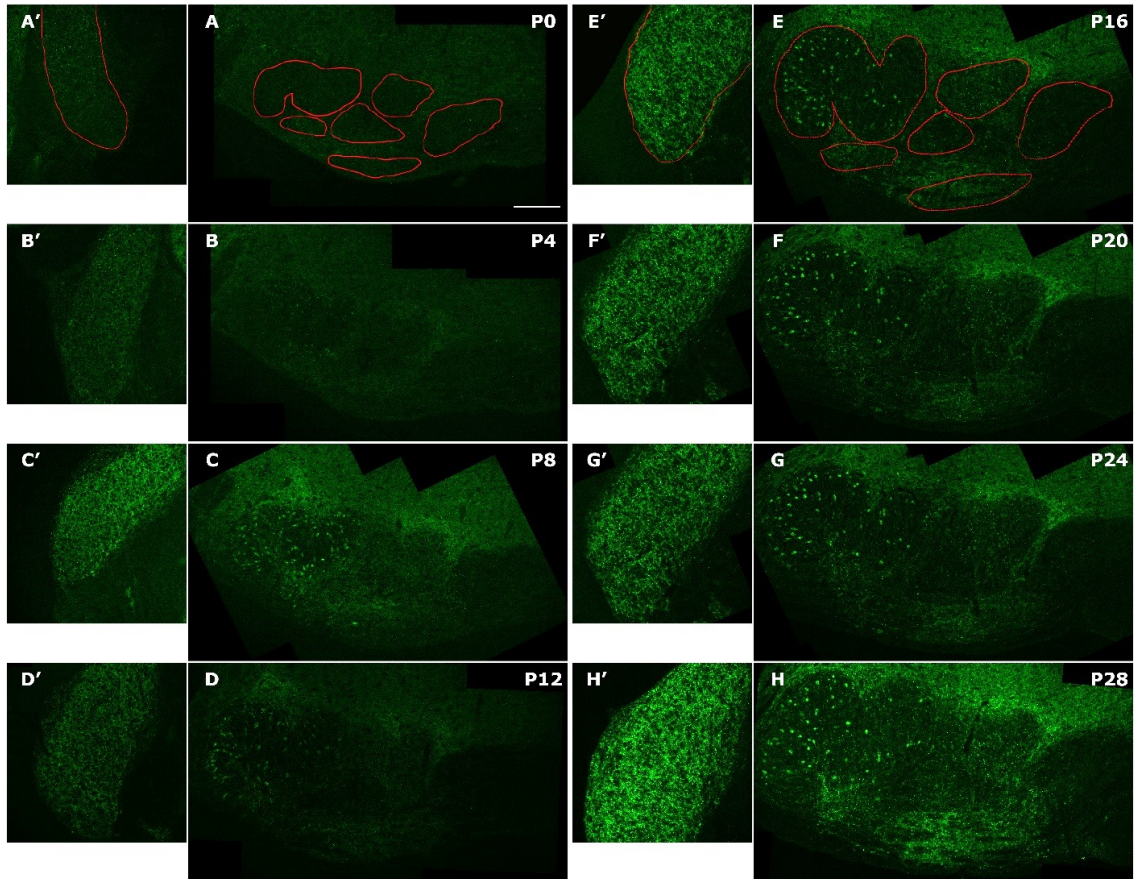


Figure 3 Overview of GAD67-IR in the developing rat SOC and VCN between P0 and P28. SOC nuclei and VCN are outlined in red (A, A', E, E'). GAD67-IR is absent in all nuclei during the first postnatal week. Almost no GAD67-IR is detected in the MNTB at any ages. Labeling in the LSO, VNTB, and VCN is detectable in the second postnatal week and increases with age (c). GAD67-IR in neuropil dorsal to the SOC also increases with age. Scale bar = 200 μm.

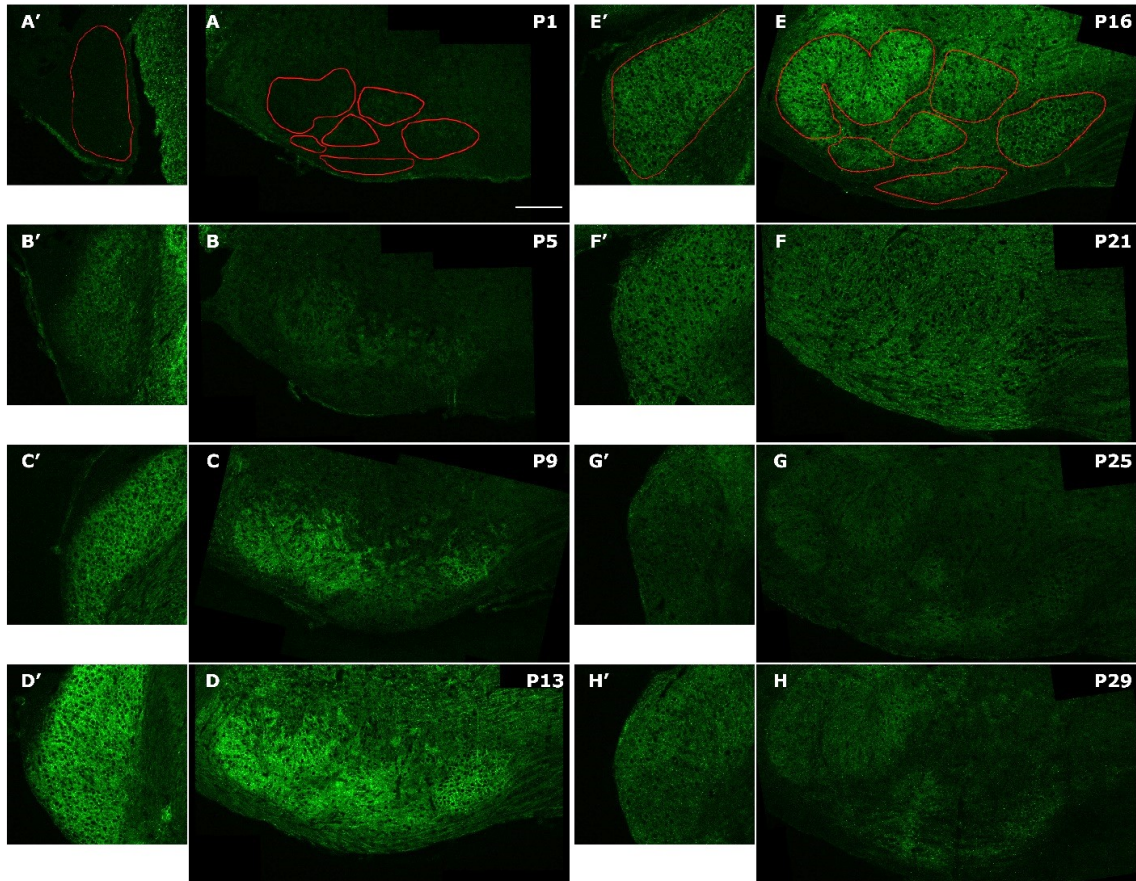


Figure 4 Overview of GAT1-IR in the developing rat SOC and VCN between P1 and P29. SOC nuclei and VCN are outlined in red (A, A', E, E'). GAT1-IR is absent in all nuclei at P1 and faintly visible at P5. GAT1-IR increases between P9 and P16 (C, D, E) then decreases almost to background levels. Labelling in the LSO, MNTB, AND SPN is not homogeneous within the nuclei between P5 and P13 (B, C, D). Scale bar = 200 μ m.

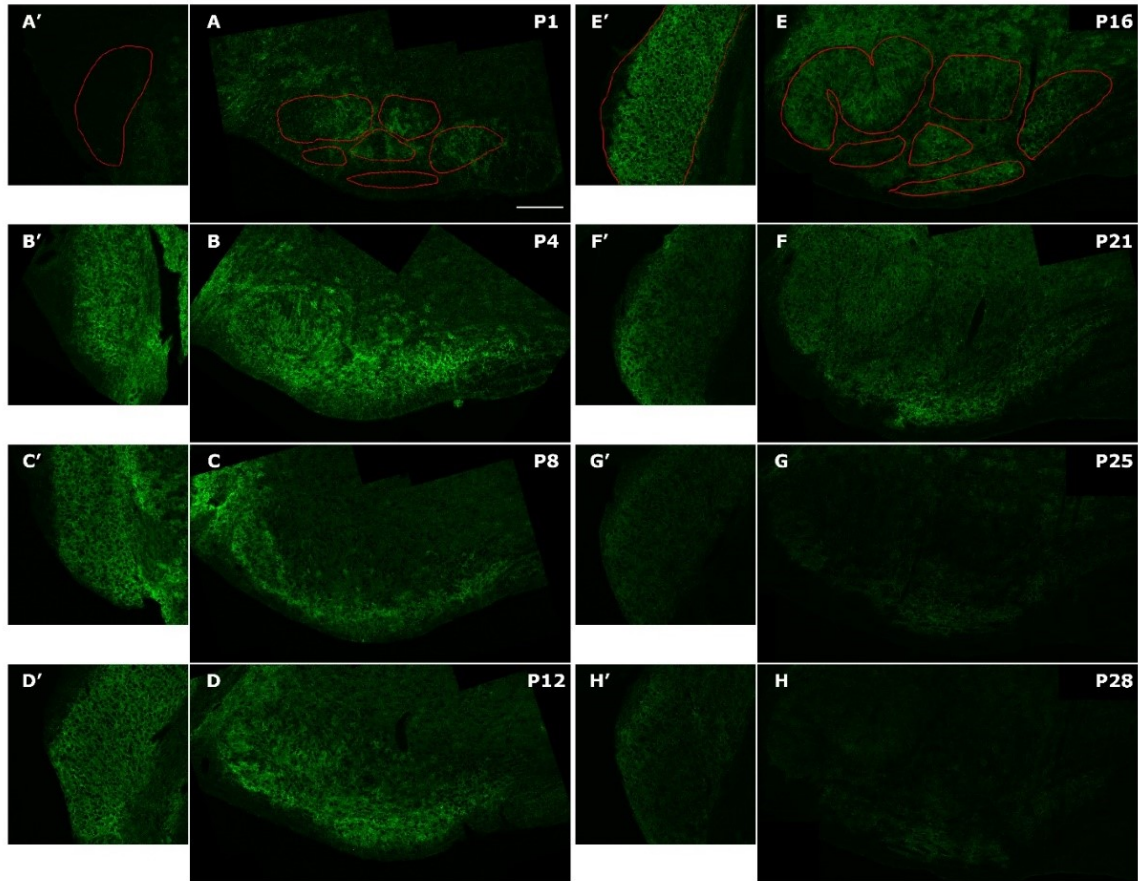


Figure 5 Overview of GAT3-IR in the developing rat SOC and VCN between P1 and P28. SOC nuclei and VCN are outlined in red (**A**, **A'**, **E**, **E'**). GAT3-IR is detectable at P1 (**a**) and peaks at P4 (**b**). GAT3-IR decreases after P4 and is absent by P28. Labelling in the LSO, MNTB, AND SPN is not homogeneous within the nuclei. Scale bar = 200 μ m.

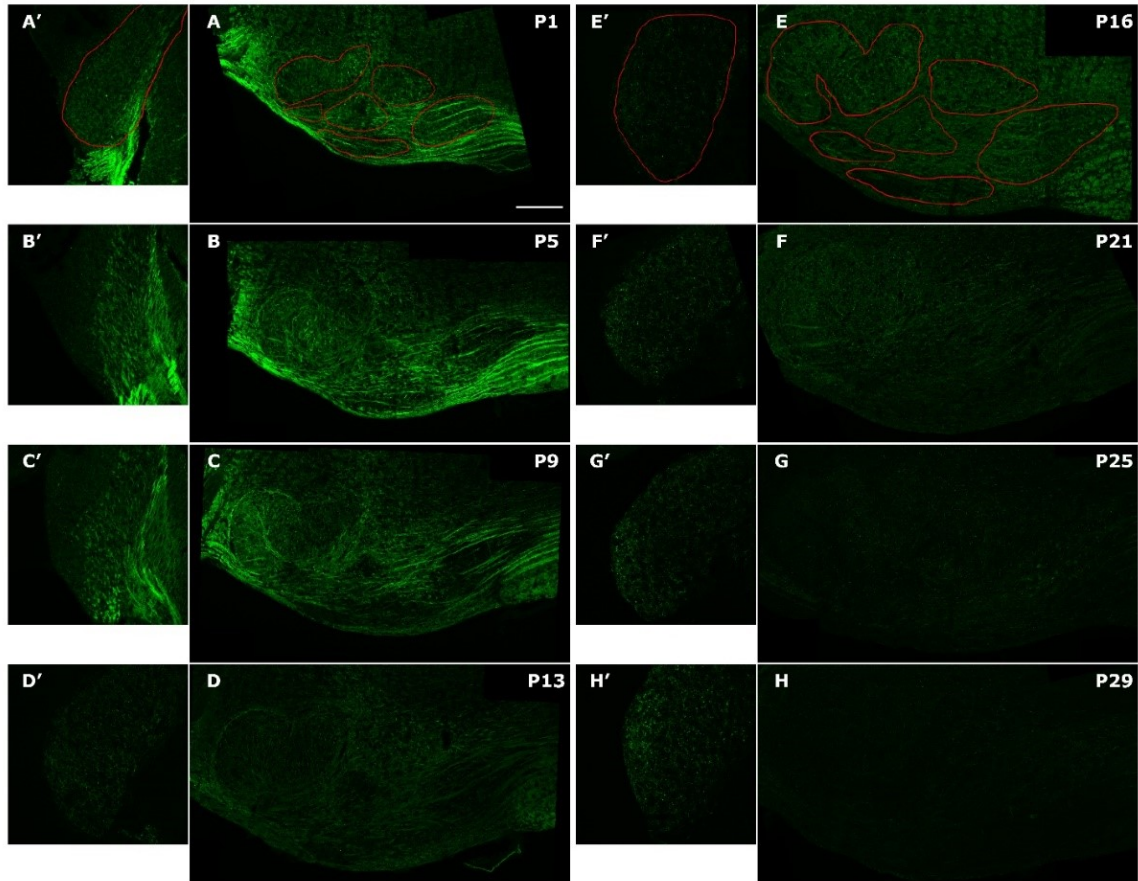


Figure 6 Overview of ALDH1A1-IR in the developing rat SOC and VCN between P1 and P29. SOC nuclei and VCN are outlined in red (**A, A', E, E'**). ALDH1A1-IR is very high during the first postnatal week (**a, b**) and decreases thereafter. ALDH1A1-IR looks fibrous and appears to course through or even to outline SOC nuclei. Scale bar = 200 μ m.

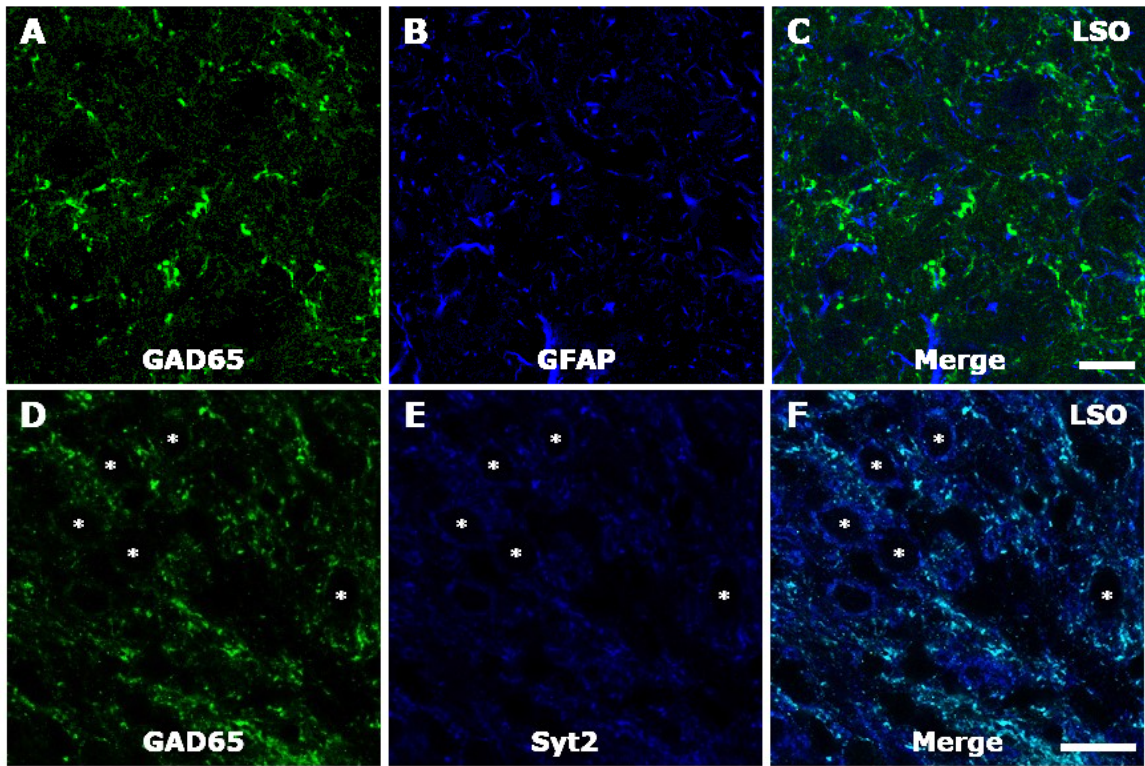


Figure 7 Single optical sections of GAD65-IR, Syt2-IR, and GFAP-IR in P16 and P21 rat tissue. Note that GAD65-IR overlaps with Syt2-IR (c; P16 tissue) in the LSO, indicating GAD65 expression in synaptic terminals. In contrast, GAD65-IR does not overlap with GFAP, indicating that GAD65 is not expressed in astrocytes (F; P21 tissue). Presumed LSO cell bodies are marked with asterisks (D, E, F). Scale bar = 50 μ m.

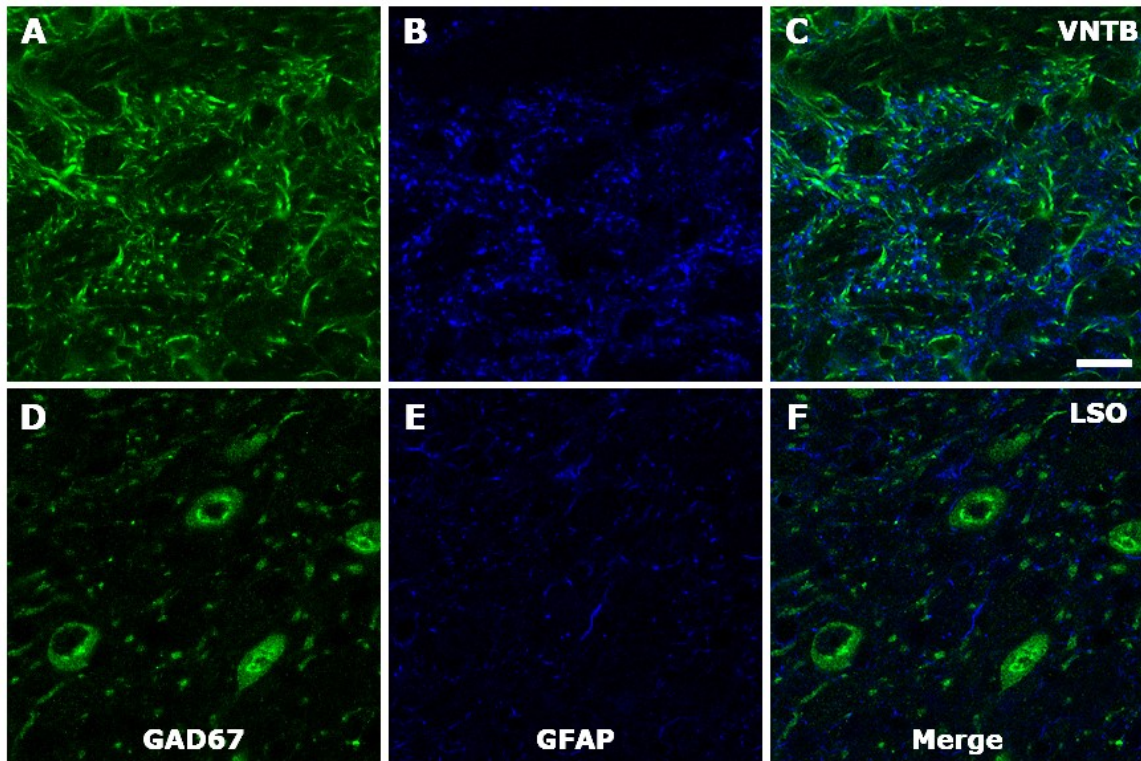


Figure 8 Single optical sections of GAD67-IR and GFAP-IR in the LSO and VNTB of P28 rat. Note that GAD67-IR does not overlap with GFAP-IR in the LSO and VNTB, indicating that GAD67 is not expressed in astrocytes (C,F). Scale bar = 50 μ m.

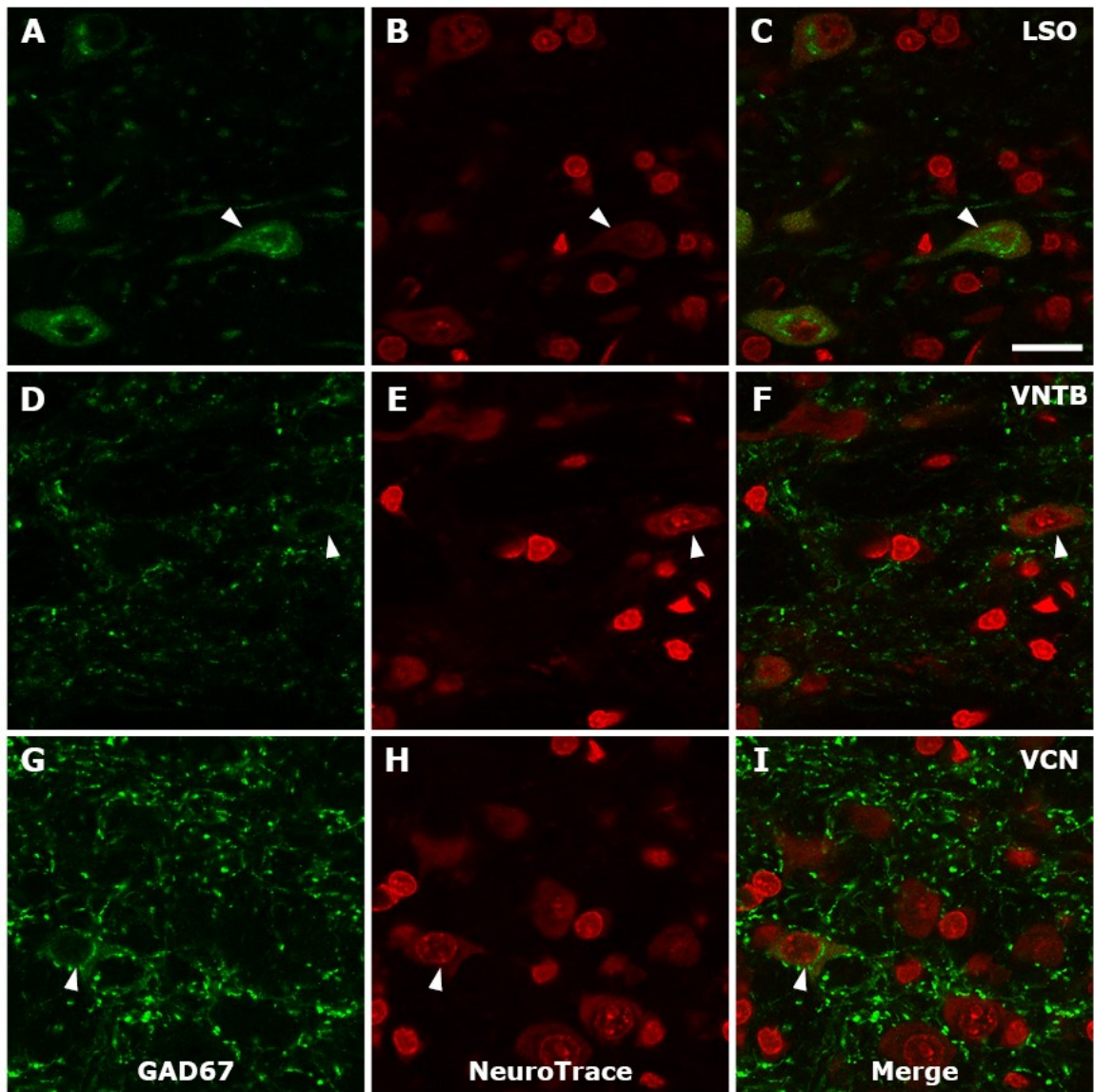


Figure 9 Single optical sections of GAD67-IR and NeuroTrace in the LSO, VNTB, and VCN of P28 rat. Note that GAD67-IR overlaps with NeuroTrace (**C, F, I**; arrow heads), indicating that the cytoplasm of LSO, VNTB, and VCN neuronal cell bodies express GAD67. In contrast, GAD67-IR is confined to cell bodies and presumably dendrites in the LSO (**C**) but is more widespread in VNTB and VCN (**F, I**). Scale bar = 50 μ m.

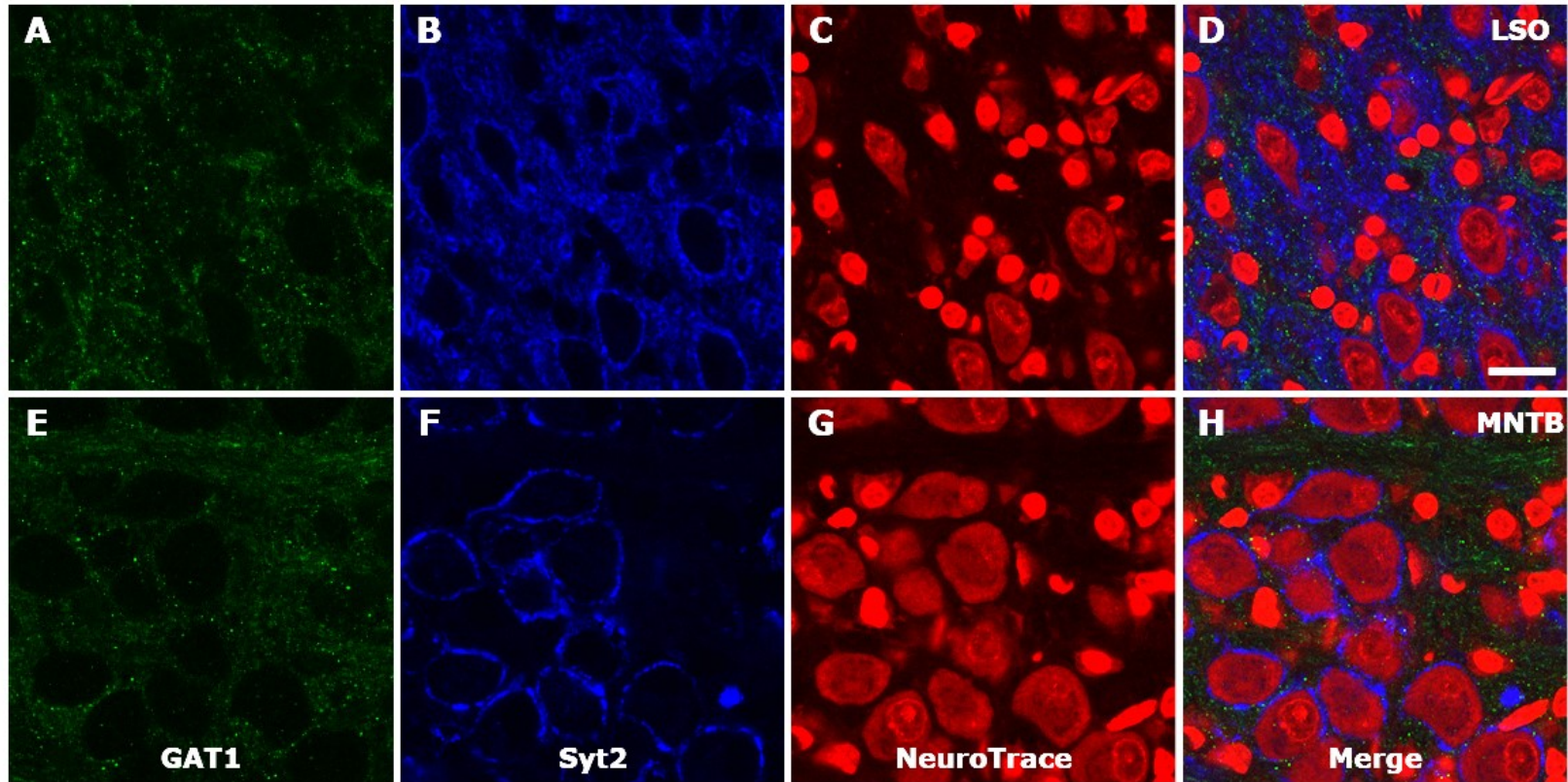


Figure 10 Single optical sections of GAT1-IR, Syt2-IR and NeuroTrace in the LSO and MNTB of P16 rat. Note the lack of overlap between GAT1-IR and Syt2-IR (**D, H**), indicating that GAT1 is not expressed in synaptic terminals. GAT1 also fails to overlap with NeuroTrace (**D, H**), indicating that neuronal cell bodies of the LSO and MNTB do not express GAT1. Scale bar = 50 μ m.

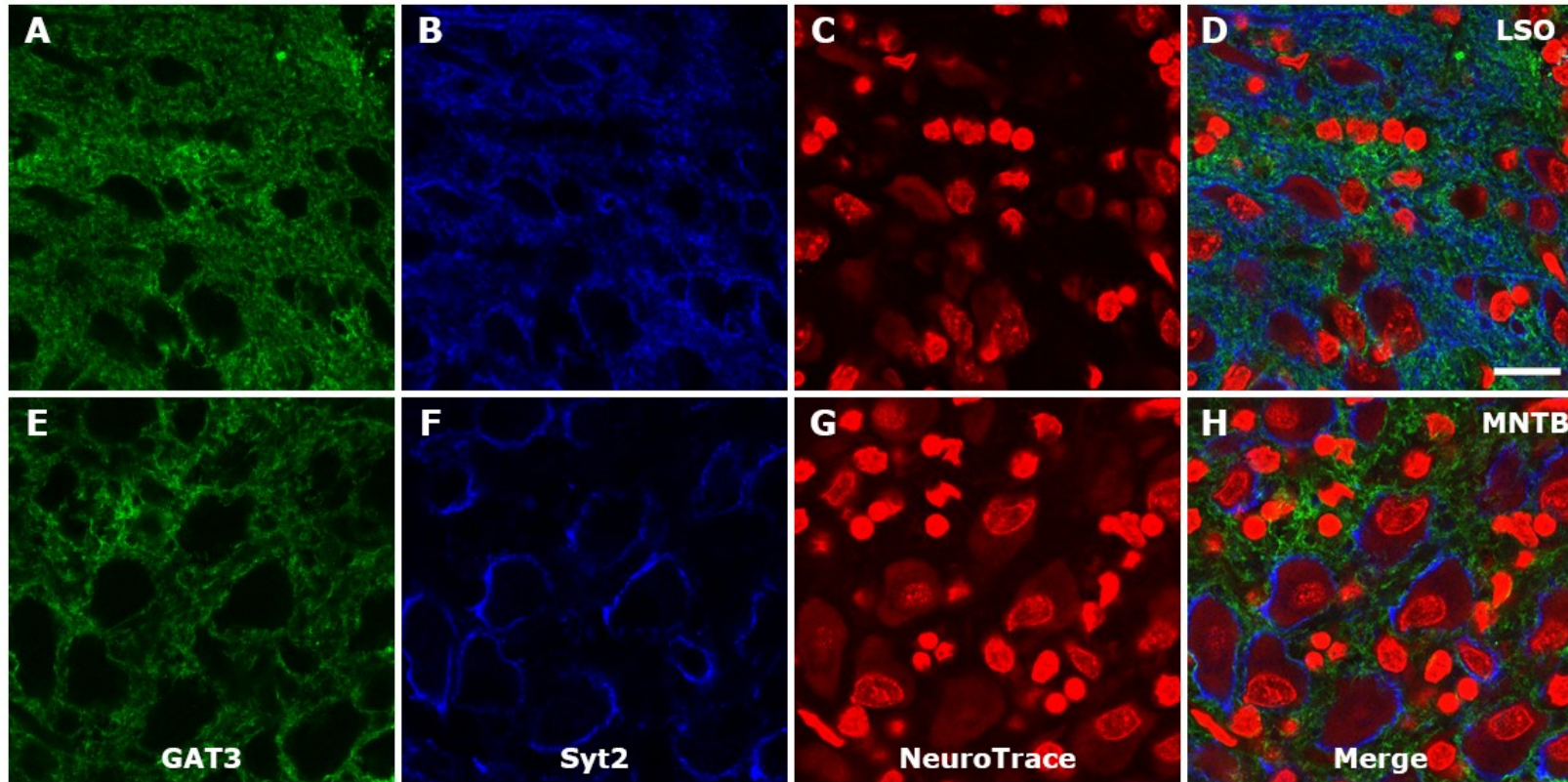


Figure 11 Single optical sections of GAT3-IR, Syt2-IR and NeuroTrace in the LSO and MNTB of P16 rat. Note the lack of overlap between GAT3-IR and Syt2-IR (**D, H**), indicating that GAT1 is not expressed in synaptic terminals. In addition, GAT3-IR also does not overlap with NeuroTrace (**D, H**), indicating a lack of GAT3 in neuronal cell bodies of the LSO and MNTB. Scale bar = 50 μm .

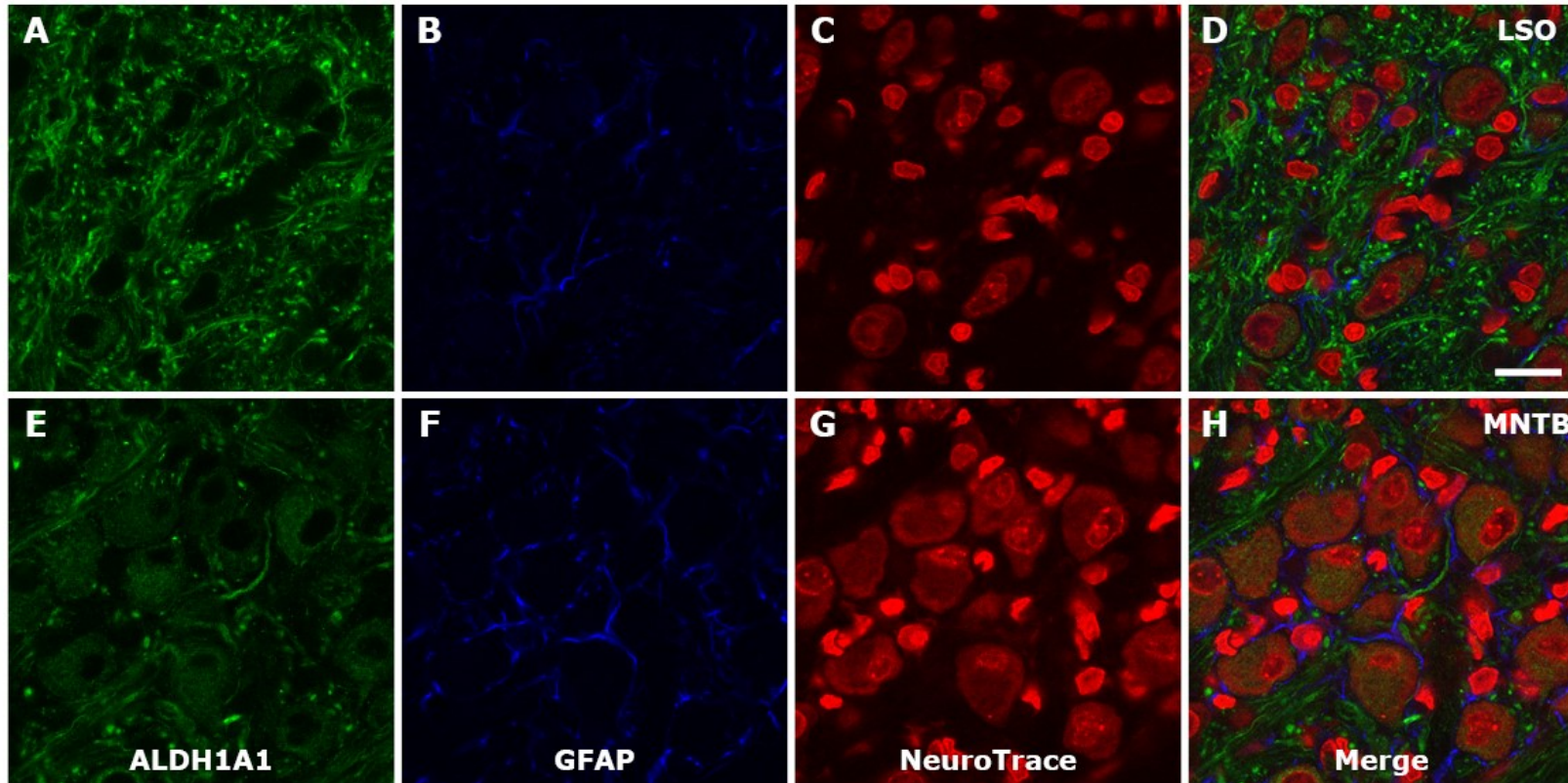


Figure 12 Single optical sections of ALDH1A1-IR, GFAP-IR, and NeuroTrace in the LSO and MNTB of P16 rat. Note the lack of overlap between ALDH1A1-IR and GFAP-IR (**D, H**), indicating that ALDH1A1 is not expressed in astrocytes. ALDH1A1-IR also fails to overlap with NeuroTrace (**D, H**), indicating a lack of ALDH1A1 expression in neuronal cell bodies of the LSO and MNTB. Scale bar = 50 μ m.

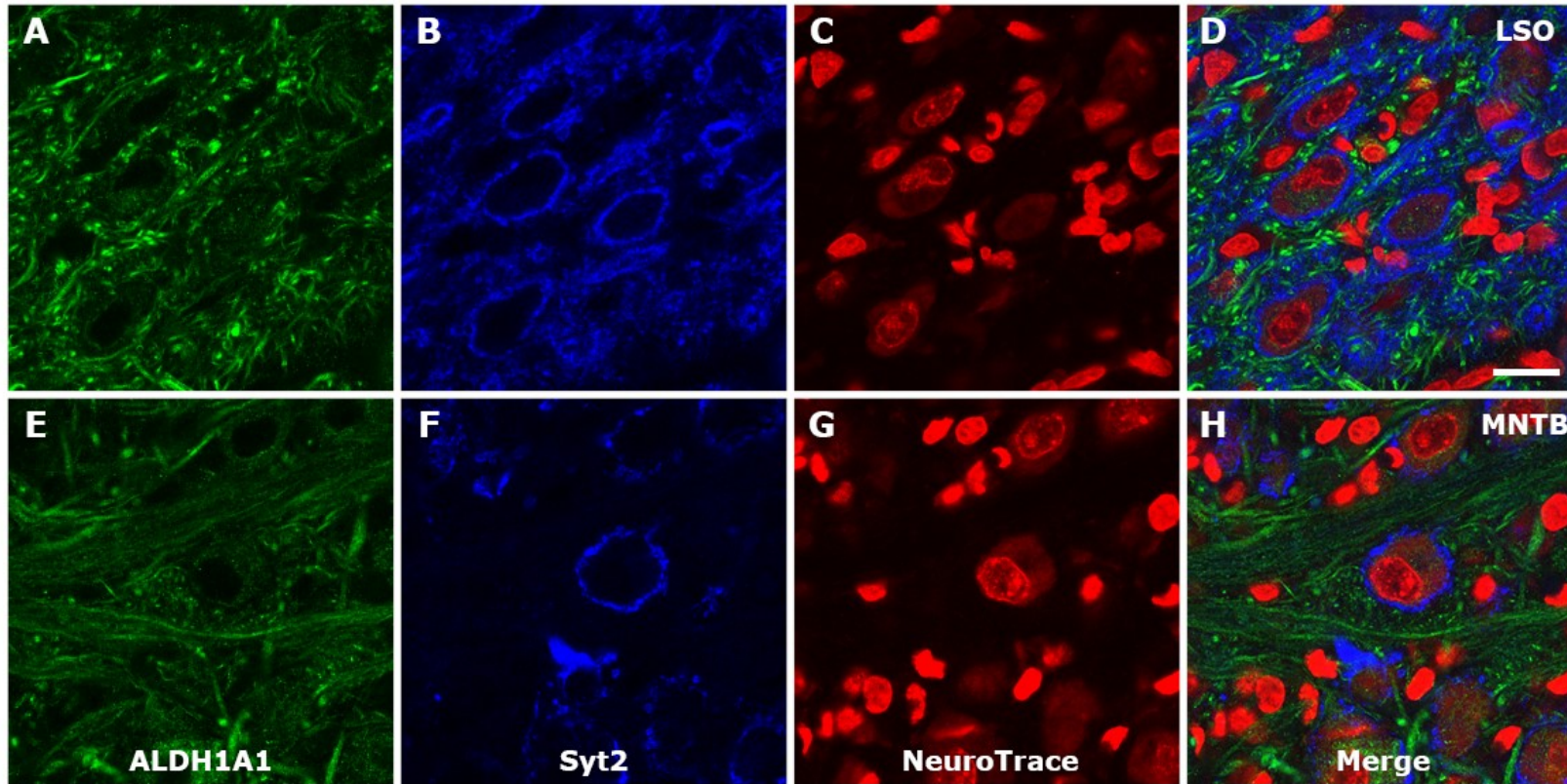


Figure 13 Single optical sections of ALDH1A1-IR, Syt2-IR, and NeuroTrace in the LSO and MNTB of P16 rat. Note the lack of overlap between ALDH1A1-IR and Syt2-IR (**D**, **H**), indicating that ALDH1A1 is not expressed in synaptic terminals. Scale bar = 50 μ m.

6. Discussion

GAD65 and GAD67 expression do not correlate with the known timeframe of GABAergic transmission in the SOC

GAD65 and GAD67 are absent in the MNTB and LSO during the period that MNTB neurons are predominantly GABAergic (Fig 2-3), suggesting that MNTB neurons may not synthesize GABA within themselves but rather acquire GABA from other sources. We know that MNTB presynaptic terminals contain GABA from EM studies in the MNTB presynaptic terminal (Nabekura et al., 2003) showing GABA immunoreactivity in the first postnatal week that decreases later. The temporal pattern of GAD65 and GAD67 does not explain the decrease in GABA content because GAD65 and GAD67 expression are elevated after the first postnatal week. GAD65 and GAD67 are also not likely to be the source of GABA in immature MNTB neurons during the first postnatal week due to their low expression.

However, the high GAD immunoreactivity in the VCN, VNTB, and LSO after P8 agrees with previous IHC studies. Roberts and Ribak (1987) found high levels of GAD-IR in the VNTB and LNTB and low levels of GAD-IR in the MNTB in adult gerbils. Albrecht et al. (2014) also detected GAD67-IR in the VNTB at P14 and adult mice, although GAD67-IR did not overlap with GlyR-IR in adults. Considering that VNTB and LNTB are glycinergic in the mature system, these results are quite interesting. Subcellular localization of GAD65 and GAD67 seen here (Fig 7-9) also agreed with Kaufman et al. (1991): GAD65 is confined to synaptic terminals and GAD67 has a more widespread expression.

In the LSO, GAD67-IR was detected in only a subset of neuronal cell bodies (Fig 3, 9C), which matched the spatial pattern in IHC experiments of Jenkins and Simmons (2006). To determine whether the GAD67-positive cells were associated with the LOC system, they used Dil to label retrogradely olivocochlear projections and found that GAD67-positive cells were also positive for the Dil label. This suggests that GAD67-positive cells in the LSO are most likely part of the LOC system.

It is also possible that GAD65 and GAD67 are present during the first postnatal week but were not detected with our methods. In situ hybridization studies by Jenkins and Simmons (2006) showed high levels of GAD65 mRNA at P5 but not GAD67. If GAD65 transcripts are present in early ages, we would also expect presence of GAD65 protein. We could perform in situ hybridization of GAD65 and GAD67 alongside IHC to verify our immunostaining results.

Non-neurotransmitter roles for GABA

Why might there be high levels of GAD enzymes later in development when there is no substantial GABAergic transmission? One possibility is that GABA can be metabolized into succinic acid and join the Krebs cycle. Reciprocally GABA can also be produced from α -ketoglutarate, a product in the Krebs cycle. GABA transaminase converts α -ketoglutarate into glutamic acid, which is then decarboxylated by GAD to form GABA. This closed loop process is known as the GABA shunt (Bown and Shelp, 1997). Plants actively metabolize GABA to maintain energy homeostasis (Michaeli and Fromm, 2015). It is conceivable that GABA formed by GAD in the presynaptic terminals may be metabolized by neighboring mitochondria and converted into an energy source, although how the neuron maintains a balance between transporting GABA into synaptic vesicles and metabolizing GABA will need to be addressed.

How might we show functionally whether GAD expression is necessary for GABAergic signalling in immature MNTB neurons? Because synaptic inputs from the MNTB are functional as early as E18 (Kandler and Friauf, 1995), we can record from GAD65-KO and/or GAD67-KO LSO neurons while stimulating the ipsilateral MNTB inputs in an acute slice to determine whether GABAergic transmission is impaired in these knockouts.

Neurons in the SOC do not express the GATs necessary for GABA uptake

(Tritsch et al., 2014) provided evidence that midbrain dopaminergic neurons can take up GABA through GATs. They detected GAT mRNA in these neurons and observed impaired GABA transmission when they applied GAT antagonists to the acute slice. These neurons cannot synthesize GABA internally as they lack GADs. To determine whether immature MNTB neurons can also take up GABA, I co-immunostained GATs with Syt2 and counterstained with NeuroTrace. Neither GAT1-IR nor GAT3-IR overlapped with either Syt2-IR or NeuroTrace (Fig 10-11H), suggesting that MNTB neurons do not express GATs in their synaptic terminals or cell bodies and therefore cannot take up GABA. In addition, I did not observe colocalization of GATs with Syt2 or NeuroTrace in other nuclei of the SOC (LSO: Fig 10-11D; other nuclei: data not shown).

GAT1 and GAT3 may be involved in GABA clearance in the SOC

Both GAT1-IR and GAT3-IR were found to be spatially close to Syt2-IR, suggesting that GATs are located very close to synaptic terminals. Subcellular localization of GATs can vary a lot between different brain regions (Scimemi, 2014) and their function is specific to where they are expressed. In cortical pyramidal neurons, GAT1 is expressed in synaptic terminals and GAT3 in astrocytes adjacent to the synaptic terminals. In

contrast, cerebellar Purkinje cells lack GAT1 and only express GAT3 in Bergmann glial cell processes surrounding the synaptic terminal. The subcellular distribution of GAT1 and GAT3 in the SOC is similar to the distribution in thalamic neurons, where both GAT1 and GAT3 are expressed in the astrocytes (Beenhakker and Huguenard, 2010). This variability in GAT expression could reflect the neuron's GABA demand. If the neuron needs a lot of GABA quickly to prevent depletion of GABA from the presynaptic terminal, the fastest path would be to directly take up GABA from the synaptic cleft rather than recycling GABA through astrocytes, whereas other inhibitory neurons may not need GABA to be replenished as quickly, and solely rely on astrocytes to recycle GABA. The subcellular distribution seen in the SOC seems to agree with the second case – GATs are only responsible for GABA clearance in the synaptic cleft by reuptake into astrocytes. The temporal pattern of GAT1 and GAT3 expression in the SOC also seems to agree with this idea. GAT3-IR is strongest during the first postnatal week (Fig 5A-B) when we see the most GABAergic transmission from immature neurons and GAT1-IR peaks in the second postnatal week (Fig 4D). Both GAT1-IR and GAT3-IR diminished by P29 (Fig 4H, 5H) when we do not expect much GABAergic transmission in the SOC circuit. In addition, Stephan and Friauf (2014) used whole-cell patch-clamp recordings with application of pharmacological agents to isolate currents from activation of GATs and glycine transporters in LSO astrocytes. Antagonists to GAT1 and GAT3 reduced GABA-evoked currents, providing functional evidence for the existence of GATs in LSO astrocytes. It would be interesting to investigate the effects of GAT antagonists on LSO postsynaptic currents from MNTB fiber stimulation in acute slices.

ALDH1A1 is potentially expressed in SOC neurons

ALDH1A1 is expressed in the cytoplasm and presumably the neurites of the SOC neurons (Fig 6, 12-13D, H) during the first two postnatal weeks. Although we can speculate that the ALDH1A1-IR seen during early development in the SOC contributes to GABA synthesis, we can extrapolate only so far on the basis of the findings presented here. The mere presence of ALDH1A1-IR does not indicate that GABA is synthesized through the putrescine degradation pathway. In addition to ALDH1A1, DAO is also required for conversion of putrescine into GABA (Seiler and Al-Therib, 1974). Midbrain dopaminergic neurons also express DAO in addition to ALDH1A1, which provides additional evidence for GABA synthesis through ALDH1A1 (Kim et al., 2015a). Therefore, we should investigate the presence of DAO and putrescine in the developing SOC.

ALDH1A1 in vitamin A metabolism

ALDH1A1 is also known as retinaldehyde dehydrogenase (RALDH) and is involved in the biosynthesis of retinoic acid from vitamin A. Retinoic acid has been implicated to

affect synaptic plasticity in some circuits (Lane and Bailey, 2005). For example, addition of retinoic acid to cultured hippocampal neurons increased synaptic transmission (Aoto et al., 2008). RALDHs are also expressed in cultured hippocampal neurons, suggesting that the neurons themselves can synthesize retinoic acid (Aoto et al., 2008).

7. Troubleshooting

Reliability of Immunohistochemistry Studies

The validity of IHC studies is a complicated topic. We have to consider the specificity of our primary and secondary antibodies to their respective targets. Although the optimal test for antibody specificity is to apply the antibody to a knockout model of the antigen in question, this is not always achievable as some genetic knockout models are not viable. I made sure to include primary deletes for each staining run and test for possible protein-protein interaction between primary and secondary antibodies when conducting co-immunostains.

Epitope masking is another common problem with IHC. Formaldehyde-fixation of tissue can create cross-linking between proteins that prevent the antibody from binding to its epitope. Prolonged exposure of tissue to fixative can greatly reduce the tissue antigenicity. Although antigen-retrieval methods exist, most of the treatment involves harsh heat and/or acid treatment that can damage tissue. There is always the possibility that the protein I am staining for is present in the tissue, but its epitopes are masked and thus I cannot visualize it using IHC. I noticed that the GAT antibodies that I used were more susceptible to fixation and required shorter fixation times.

Glial Expression in the SOC

GFAP-IR was not observed in the SOC until the second postnatal week. This proved problematic as I was focussed on the subcellular distributions of GADs, GATs, and ALDH1A1 during the first postnatal week. (Cahoy et al., 2008) reported that ALDH1L1 is a highly specific astrocyte marker with a broader pattern of expression than GFAP. This was also confirmed in the brainstem by (Dinh et al., 2014). They observed ALDH1L1-IR in major SOC nuclei at P0 but not GFAP-IR. Therefore, I do not have solid evidence that GABA synthesis and transport proteins are not expressed in astrocytes if GFAP-IR does not reliably reveal astrocytes early in development.

ALDH1A1 Antibody Specificity

I discovered after completing my experiments that the particular ALDH1A1 antibody (cat# ab23375) I used has been discontinued. Abcam states that after evaluation of the antibody using A549 knockout cell lines, they discovered that ab23375 did not react specifically with the target protein.

8. Conclusion

Historically GADs have been used as a marker for GABAergic neurons. Here we show that immature GABAergic neurons of the MNTB do not express GAD65 and GAD67, raising the possibility that immature glycinergic terminals of the auditory brainstem may acquire GABA through GATs or synthesis mediated by ALDH1A1, as reported in midbrain dopaminergic neurons. Although I did observe evidence of ALDH1A1 but not GATs in SOC neurons, further functional and in situ hybridization studies should be conducted to verify my IHC results.

REFERENCES

Akerman CJ, Cline HT (2006) Depolarizing GABAergic Conductances Regulate the Balance of Excitation to Inhibition in the Developing Retinotectal Circuit In Vivo. *J Neurosci* 26:5117–5130.

Albrecht O, Dondzillo A, Mayer F, Thompson JA, Klug A (2014) Inhibitory projections from the ventral nucleus of the trapezoid body to the medial nucleus of the trapezoid body in the mouse. *Frontiers in Neural Circuits* 8:83.

Aoto J, Nam CI, Poon MM, Ting P, Chen L (2008) Synaptic Signaling by All-Trans Retinoic Acid in Homeostatic Synaptic Plasticity. *Neuron* 60:308–320.

Asada H, Kawamura Y, Maruyama K, Kume H, Ding R-G, Kanbara N, Kuzume H, Sanbo M, Yagi T, Obata K (1997) Cleft palate and decreased brain γ -aminobutyric acid in mice lacking the 67-kDa isoform of glutamic acid decarboxylase. *Proc National Acad Sci* 94:6496–6499.

Asada H, Kawamura Y, Maruyama K, Kume H, Ding R, Ji F, Kanbara N, Kuzume H, Sanbo M, Yagi T, Obata K (1996) Mice Lacking the 65 kDa Isoform of Glutamic Acid Decarboxylase (GAD65) Maintain Normal Levels of GAD67 and GABA in Their Brains but Are Susceptible to Seizures. *Biochem Biophys Res Commun* 229:891–895.

Avila A, Nguyen L, Rigo J-M (2013) Glycine receptors and brain development. *Front Cell Neurosci* 7:184.

Beenhakker MP, Huguenard JR (2010) Astrocytes as Gatekeepers of GABAB Receptor Function. *J Neurosci* 30:15262–15276.

Borden LA (1996) GABA Transporter Heterogeneity: Pharmacology and Cellular Localization. *Neurochem Int* 29:335–356.

Boudreau J, Tsuchitani C (1968) Binaural interaction in the cat superior olive S segment. *Journal of neurophysiology* 31:442–454.

Bown A, Shelp B (1997) The Metabolism and Functions of γ -Aminobutyric Acid. *Plant Physiol* 115:1–5.

Cahoy JD, Emery B, Kaushal A, Foo LC, Zamanian JL, Christopherson KS, Xing Y, Lubischer JL, Krieg PA, Krupenko SA, Thompson WJ, Barres BA (2008) A Transcriptome Database for Astrocytes, Neurons, and Oligodendrocytes: A New Resource for Understanding

Brain Development and Function. *J Neurosci* 28:264–278.

Caird D, Klinke R (1983) Processing of binaural stimuli by cat superior olivary complex neurons. *Experimental brain research* 52:385–399.

Cant N, Hyson RL (1992) Projections from the lateral nucleus of the trapezoid body to the medial superior olivary nucleus in the gerbil. *Hearing Res* 58:26–34.

Case DT, Gillespie DC (2011) Pre- and postsynaptic properties of glutamatergic transmission in the immature inhibitory MNTB-LSO pathway. *Journal of neurophysiology* 106:2570–2579.

Case DT, Zhao X, Gillespie DC (2011) Functional Refinement in the Projection from Ventral Cochlear Nucleus to Lateral Superior Olive Precedes Hearing Onset in Rat. *PLoS ONE* 6:e20756.

Chang EH, Kotak VC, Sanes DH (2003) Long-Term Depression of Synaptic Inhibition Is Expressed Postsynaptically in the Developing Auditory System. *Journal of Neurophysiology* 90:1479–1488.

Chang Y, Gottlieb D (1988) Characterization of the proteins purified with monoclonal antibodies to glutamic acid decarboxylase. *J Neurosci* 8:2123–2130.

Darrow KN, Benson TE, Brown CM (2012) Planar multipolar cells in the cochlear nucleus project to medial olivocochlear neurons in mouse. *J Comp Neurol* 520:1365–1375.

Dinh ML, Koppel SJ, Korn MJ, Cramer KS (2014) Distribution of glial cells in the auditory brainstem: Normal development and effects of unilateral lesion. *Neuroscience* 278.

Doucet JR, Ryugo DK (2006) Structural and functional classes of multipolar cells in the ventral cochlear nucleus. *The Anatomical Record Part A: Discoveries in Molecular, Cellular, and Evolutionary Biology* 288A:331–344.

Dumoulin A, Triller A, Dieudonné S (2001) IPSC Kinetics at Identified GABAergic and Mixed GABAergic and Glycinergic Synapses onto Cerebellar Golgi Cells. *J Neurosci* 21:6045–6057.

Erlander M, Tillakaratne N, Feldblum S, Patel N, Tobin A (1991) Two genes encode distinct glutamate decarboxylases. *Neuron* 7:91–100.

Fong AY, Stornetta RL, Foley C, Potts JT (2005) Immunohistochemical localization of

GAD67-expressing neurons and processes in the rat brainstem: subregional distribution in the nucleus tractus solitarius. *The Journal of comparative neurology* 493:274–290.

Forsythe I (1994) Direct patch recording from identified presynaptic terminals mediating glutamatergic EPSCs in the rat CNS, in vitro. *J Physiology* 479:381–387.

Fox MA, Sanes JR (2007) Synaptotagmin I and II are present in distinct subsets of central synapses. *J Comp Neurol* 503:280–296.

Gamlin CR, Yu W-Q, Wong RO, Hoon M (2018) Assembly and maintenance of GABAergic and Glycinergic circuits in the mammalian nervous system. *Neural Development* 13:12.

Ge S, Goh EL, Sailor KA, Kitabatake Y, Ming G, Song H (2005) GABA regulates synaptic integration of newly generated neurons in the adult brain. *Nature* 439:589–593.

Grothe B, Pecka M, McAlpine D (2010) Mechanisms of sound localization in mammals. *Physiological reviews* 90:983–1012.

Harris JJ, Jolivet R, Attwell D (2012) Synaptic Energy Use and Supply. *Neuron* 75:762–777.

Hassfurth B, Grothe B, Koch U (2010) The Mammalian Interaural Time Difference Detection Circuit Is Differentially Controlled by GABAB Receptors during Development. *J Neurosci* 30:9715–9727.

Helfert RH, Schwartz IR (1987) Morphological features of five neuronal classes in the gerbil lateral superior olive. *American Journal of Anatomy* 179:55–69.

Hirtz JJ, Braun N, Griesemer D, Hannes C, Janz K, Löhrke S, Müller B, Friauf E (2012) Synaptic refinement of an inhibitory topographic map in the auditory brainstem requires functional Cav1.3 calcium channels. *The Journal of neuroscience: the official journal of the Society for Neuroscience* 32:14602–14616.

Ikegaki N, Saito N, Hashima M, Tanaka C (1994) Production of specific antibodies against GABA transporter subtypes (GAT1, GAT2, GAT3) and their application to immunocytochemistry. *Mol Brain Res* 26:47–54.

Ito S (2016) GABA and glycine in the developing brain. *J Physiological Sci* 66:375–379.

Jenkins S, Simmons D (2006) GABAergic neurons in the lateral superior olive of the hamster are distinguished by differential expression of gad isoforms during

development. *Brain research* 1111:12–25.

Johnson J, Chen T, Rickman D, Evans C, Brecha N (1996) Multiple gamma-Aminobutyric acid plasma membrane transporters (GAT-1, GAT-2, GAT-3) in the rat retina. *The Journal of comparative neurology* 375:212–224.

Kadner A, Kulesza RJ, Berrebi AS (2006) Neurons in the Medial Nucleus of the Trapezoid Body and Superior Paraolivary Nucleus of the Rat May Play a Role in Sound Duration Coding. *J Neurophysiol* 95:1499–1508.

Kandler K, Friauf E (1995) Development of glycinergic and glutamatergic synaptic transmission in the auditory brainstem of perinatal rats. *The Journal of neuroscience : the official journal of the Society for Neuroscience* 15:6890–6904.

Kanold PO, Shatz CJ (2006) Subplate Neurons Regulate Maturation of Cortical Inhibition and Outcome of Ocular Dominance Plasticity. *Neuron* 51:627–638.

Kaufman DL, Houser CR, Tobin AJ (1991) Two Forms of the γ -Aminobutyric Acid Synthetic Enzyme Glutamate Decarboxylase Have Distinct Intraneuronal Distributions and Cofactor Interactions. *Journal of Neurochemistry* 56:720–723.

Kim D, Deerinck TJ, gal Y, Babcock HP, Ellisman MH, Zhuang X (2015a) Correlative Stochastic Optical Reconstruction Microscopy and Electron Microscopy. *PLOS ONE* 10:e0124581.

Kim J-I, Ganesan S, Luo SX, Wu Y-W, Park E, Huang EJ, Chen L, Ding JB (2015b) Aldehyde dehydrogenase 1a1 mediates a GABA synthesis pathway in midbrain dopaminergic neurons. *Science* 350:102–106.

Konur S, Ghosh A (2005) Calcium Signaling and the Control of Dendritic Development. *Neuron* 46:401–405.

Kopp-Scheinpflug C, Tozer A, Robinson SW, Tempel BL, Hennig MH, Forsythe ID (2011) The Sound of Silence: Ionic Mechanisms Encoding Sound Termination. *Neuron* 71:911–925.

Kopp-Scheinpflug C, Forsythe ID (2018). GS (1981) Integration of synaptic and intrinsic conductances shapes microcircuits in the superior olivary complex. In: *The Mammalian Auditory Pathways: Synaptic Organization and Microcircuits* (Oliver DL, Cant NB, Fay RR, Popper AN, ed), pp101–126. Cham, Switzerland: Springer.

Korada S, Schwartz I (1999) Development of GABA, glycine, and their receptors in the auditory brainstem of gerbil: a light and electron microscopic study. *The Journal of comparative neurology* 409:664–681.

Kotak V, Korada S, Schwartz I, Sanes D (1998) A developmental shift from GABAergic to glycinergic transmission in the central auditory system. *The Journal of neuroscience : the official journal of the Society for Neuroscience* 18:4646–4655.

Kullmann PH, Ene AF, Kandler K (2002) Glycinergic and GABAergic calcium responses in the developing lateral superior olive. *European Journal of Neuroscience* 15:1093–1104.

Kuwabara N, DiCaprio R, Zook JM (1991) Afferents to the medial nucleus of the trapezoid body and their collateral projections. *J Comp Neurol* 314:684–706.

Lane MA, Bailey SJ (2005) Role of retinoid signalling in the adult brain. *Prog Neurobiol* 75:275–293.

Lee H, Bach E, Noh J, Delpire E, Kandler K (2016) Hyperpolarization-independent maturation and refinement of GABA/glycinergic connections in the auditory brain stem. *Journal of Neurophysiology* 115:1170–1182.

Michaeli S, Fromm H (2015) Closing the loop on the GABA shunt in plants: are GABA metabolism and signaling entwined? *Front Plant Sci* 6:419.

Nabekura J, Katsurabayashi S, Kakazu Y, Shibata S, Matsubara A, Jinno S, Mizoguchi Y, Sasaki A, Ishibashi H (2003) Developmental switch from GABA to glycine release in single central synaptic terminals. *Nature Neuroscience* 7:17–23.

Noh J, Seal RP, Garver JA, Edwards RH, Kandler K (2010) Glutamate co-release at GABA/glycinergic synapses is crucial for the refinement of an inhibitory map. *Nature neuroscience* 13:232–238.

Roberts E, Frankel S (1951) Further studies of glutamic acid decarboxylase in brain. *J Biological Chem* 190:505–512.

Roberts R, Ribak C (1987) GABAergic neurons and axon terminals in the brainstem auditory nuclei of the gerbil. *The Journal of comparative neurology* 258:267–280.

Rubio, M (2018). Microcircuits of the Ventral Cochlear Nucleus. In: *The Mammalian Auditory Pathways: Synaptic Organization and Microcircuits* (Oliver DL, Cant NB, Fay RR, Popper AN, ed), pp41-73. Cham, Switzerland: Springer.

Sanes D, Siverls V (1991) Development and specificity of inhibitory terminal arborizations in the central nervous system. *Journal of neurobiology* 22:837–854.

Sanes D, Takács C (1993) Activity-dependent refinement of inhibitory connections. *The European journal of neuroscience* 5:570–574.

Scimemi A (2014) Structure, function, and plasticity of GABA transporters. *Front Cell Neurosci* 8:161.

Seiler N, Al-Therib M (1974) Putrescine catabolism in mammalian brain. *Biochem J* 144:29–35.

Spirou GA, Rowland KC, Berrebi AS (1998) Ultrastructure of neurons and large synaptic terminals in the lateral nucleus of the trapezoid body of the cat. *J Comp Neurol* 398:257–272.

Stephan J, Friauf E (2014) Functional analysis of the inhibitory neurotransmitter transporters GlyT1, GAT-1, and GAT-3 in astrocytes of the lateral superior olive. *Glia* 62:1992–2003.

Tian N, Petersen C, Kash S, Baekkeskov S, Copenhagen D, Nicoll R (1999) The role of the synthetic enzyme GAD65 in the control of neuronal γ -aminobutyric acid release. *Proceedings of the National Academy of Sciences* 96:12911–12916.

Trevarrow B, Marks DL, Kimmel CB (1990) Organization of hindbrain segments in the zebrafish embryo. *Neuron* 4:669–679.

Tritsch NX, Oh W-J, Gu C, Sabatini BL (2014) Midbrain dopamine neurons sustain inhibitory transmission using plasma membrane uptake of GABA, not synthesis. *eLife* 3:e01936.

Warr WB, Beck J (1996) Multiple projections from the ventral nucleus of the trapezoid body in the rat. *Hearing Research* 93:83–101.